All the PNS is a Stage: Transplanted Bone Marrow Cells Play an Immunomodulatory Role in Peripheral Nerve Regeneration

Gonzalo Piñero[1,2,3], Marianela Vence[2], Marcos L. Aranda[4,5], Magalí C. Cercato[2], Paula A. Soto[1,2], Vanina Usach[1,2] and Patricia C. Setton-Avruj[1,2] (iD)

Abstract

Working on a Wallerian degeneration model in rats, our group has shown the beneficial effects of systemic bone marrow mononuclear cell transplant on morphological and functional parameters, as well as the prevention of neuropathic pain. The current work thus seeks to evaluate the effect of systemic bone marrow cell transplant in a mouse model of sciatic nerve crush and aims to dig deeper into the mechanisms involved in bone marrow cell therapy. Adult C57BL/6J mice were subjected to 8s sciatic nerve crush and intravenously transplanted with bone marrow cells. Cells were tracked using a fluorescent probe, and the evolution of the degeneration–regeneration process was evaluated through axonal and myelin marker immunodetection at different survival times. Gene and protein expression of the main cytokines involved in the inflammatory phase and lesion-associated macrophage phenotypes were also analyzed. Initial findings corroborated the beneficial effect of bone marrow cells on the regenerative process and proved their efficiency in reducing the expression of some proinflammatory cytokines and increasing that of anti-inflammatory interleukin 10 (IL-10). In addition, transplanted animals showed a decrease in inducible nitric oxide synthase (iNOS)$^+$ macrophages, an increment in CD206$^+$ cells, and an anticipated rise in Arg-1$^+$ macrophages. Taken together, our results endorse bone marrow cell therapy as an alternative approach to accelerate nerve recovery and postulate bone marrow cells as potential immunomodulators.

Summary Statement

Bone marrow cell transplant has proven to be an effective therapeutic approach to treat peripheral nervous system injuries as it not only promoted regeneration and remyelination of the injured nerve but also had a potent effect on neuropathic pain.

Keywords

Wallerian degeneration, bone marrow cells, remyelination, immunomodulation

Received September 22, 2022; Revised February 28, 2023; Accepted for publication March 16, 2023

[1]Departamento de Química Biológica, Cátedra de Química Biológica Patalógica, Facultad de Farmacia y Bioquímica, Universidad de Buenos Aires, Ciudad Autónoma de Buenos Aires, Argentina

[2]Universidad de Buenos Aires-CONICET, Instituto de Química y Fisicoquímica Biológicas (IQUIFIB), Ciudad Autónoma de Buenos Aires, Argentina

[3]Department of Pathology, Mount Sinai Hospital, New York, NY, USA

[4]Universidad de Buenos Aires-CONICET, Centro de Estudios Farmacológicos y Botánicos (CEFYBO), Ciudad Autónoma de Buenos Aires, Argentina

[5]Department of Neurobiology, Weinberg College of Arts and Sciences, Northwestern University, Evanston, IL, USA

After all the years sharing research and life with Giannina, there are many things we can highlight about her: tireless worker, dedicated teacher, and a woman of strong personality. However, there is something all the scientists who worked with her can agree on: her passion for science, which transcends and is worthy of admiration. Without a doubt, she built a successful career, guide many of us along the way and left and still keeps leaving a mark in our field.

Corresponding Author:
Patricia C. Setton-Avruj. Cátedra de Química Biológica Patológica, Facultad de Farmacia y Bioquímica, Universidad de Buenos Aires. Junín 956, 5th floor, CP1113, Ciudad Autónoma de Buenos Aires, Argentina.
Email: setton@qb.ffyb.uba.ar

Introduction

The loss of axonal integrity upon peripheral nerve lesion alters axon-Schwann cell (SC) contact and triggers Wallerian degeneration (WD). In this scenario, SCs actively proliferate and acquire a repairing phenotype characterized by their ability to digest myelin through autophagy and receptor-mediated phagocytosis (Gomez-Sanchez et al., 2015; Lutz et al., 2017) and to secrete trophic factors and cytokines which promote neuronal survival and leukocyte influx (Jessen & Arthur-Farraj, 2019). Activated SCs also initiate a potent inflammatory response that involves leukocyte infiltration. Over the first hours, neutrophils are the main hematogenous population but, after 48 to 72 h, the influx of monocytes notably increases. Together with nerve-associated macrophages (Kolter et al., 2020), these monocytes assume a key role in the immune response and actively participate in cell and myelin debris removal (DeFrancesco-Lisowitz et al., 2015; Kalinski et al., 2020; Liu et al., 2019). The interaction of SCs, fibroblasts, axons, and immune cells establishes a microenvironment supportive of axonal regeneration and remyelination. However, nerve function recovery is still a major concern.

In recent years, cell transplantation techniques have received special attention given their potential application in regenerative therapies. Although the sources from which cells can be obtained may greatly vary, bone marrow cells (BMCs), an heterogeneous population that include hematopoietic progenitor cells, myeloid and lymphoid precursors, endothelial progenitor cells, and mesenchymal stem cells (Abreu et al., 2014; Goel et al., 2009), have shown a positive impact in various models of nerve injury such as transection (Goel et al., 2009; Muheremu et al., 2017; Ribeiro-Resende et al., 2009, 2012) and compression (Zaverucha-do-Valle et al., 2011, 2014), as well as diabetic peripheral neuropathy (Kim et al., 2009; Mao et al., 2019; Naruse et al., 2011). In a reversible WD model, it had been demonstrated that systemically transplanted bone marrow mononuclear cells migrate to the lesion area and promote axonal regeneration and remyelination, improving functional recovery and preventing neuropathic pain (Usach et al., 2011, 2017). It has also been shown that the majority of systemically transplanted cells resemble host immune cell migration patterns and also participate in myelin clearance, while a small proportion undergoes phenotypic changes at the end of the regenerative process (Piñero et al., 2018). Although data on the mechanisms underlying the effect of BMCs on sciatic nerve injury remain scarce, our previous results indicate that transplanted cells may play additional roles such as the modulation of the inflammatory response in WD.

In this context, the aim of the present work was to evaluate the potential immunomodulatory effect of BMC transplantation and its regenerative impact on nerve morphology and function in a mouse model of WD. Analyses were carried out on the distribution and levels of myelin basic protein

Table 1. Materials and Reagents Used.

Brand	Material/reagent	Catalog number
Thermo Fisher Scientific	DMEM	12800017
	Trizol	15596026
	MicroAmp 96-well plates	N8010560
	SYBR Green Master Mix® PowerUp kit	A25742
	UltraComp eBeads	01-2222
	Ortho-phenylenediamine	34006
Serendipia Lab	Fetal calf serum	
Zymo Research	RNA Clean & Concentrator-5 Spin-Columns	R1015
Promega	MMLV–RT	M1701
Biodynamics	OligodT	B07-40
	dNTPs	U1330
Worthington Biochemicals	Collagenase IV	LS004186
	DNAse I	LS002004
Biologend	Zombie yellow	423103
	CFSE	423801
Biopack	Saponin	2000946000
	Tween 20	2000200300
	H$_2$O$_2$	2000980300
Millipore Sigma	Protease Inhibitor Cocktail Set III	535140
	Triton X-100	X100
	DAPI	D942
	Paraformaldehyde	158127
	Mowiol 4-88	81381
Corning	Polystyrene high bind plate	3590

Notes. CFSE: carboxyfluoresceinsuccinimidyl ester; DAPI: 4′,6-diamidino-2-phenylindole; DMEM: Dulbecco's modified Eagle's medium; dNTP: deoxynucleoside triphosphate; MMLV–RT: Moloney murine leukemia virus reverse transcriptase.

(MBP), a major myelin protein highly sensitive to WD, and bIII-tubulin, a cytoskeletal protein useful to evaluate axonal integrity. In addition, two different tests to assess the functional recovery of the injured sciatic nerve were used. To confirm whether this effect is mediated by immunomodulation, representative cytokine profiles and lesion-associated macrophage phenotypes were evaluated.

Materials and Methods

Materials

All reagents used in this work are listed in Table 1.

Sciatic Nerve Injury

All animals used in this study were treated humanely and all procedures were performed in accordance with the guidelines of the Committee of Bioethics at Facultad de Farmacia y

Bioquímica, Universidad de Buenos Aires (CICUAL-FFyB; Exp. 68987/2017; Res. CD2651/2018) and following the NIH Guide for the Care and Use of Laboratory Animals and EU Directive 2010/63/EU for animal experiments of the European Commission.

C57BL/6J mice were housed in standard cages in a temperature-controlled room ($22°C \pm 2°C$) on a 12 h light-dark cycle. Food and water were provided *ad libitum*. Eight-week-old to 10-week-old male mice were divided into three experimental groups: nerve lesion plus vehicle injection (non-treated), nerve lesion plus BMC transplant (treated), and a control group given by exposed nonlesioned nerves (sham). Mice were anesthetized with intraperitoneal (i.p.) 110 mg/kg ketamine and 10 mg/kg xylazine, and their right sciatic nerves—from now on referred to as ipsilateral nerves—were exposed and crushed for 8 s at mid-thigh level with #5 tweezers. Upon compression, two areas were defined in each ipsilateral nerve: the proximal stump, extending from dorsal root ganglia to the lesion site; and the distal stump, from the crush area to the end of the nerve. Left non-lesioned nerves—from now on referred to as contralateral nerves—were used as internal controls.

BMC Isolation

Femurs and tibias were dissected from eight-week-old to 10-week-old female C57BL/6J mice. The bone marrow was extruded with Dulbecco's modified Eagle's medium (DMEM) supplemented with 10% fetal calf serum (FCS). Bone marrow aspirates were mechanically disaggregated by pipetting up and down and then centrifuged (300 x g, 10 min, room temperature [RT]). Cells were resuspended in erythrocytes lysis buffer (150 mM NH_4Cl, 10 mM $NaHCO_3$, 1 mM ethylenediaminetetraacetic acid [EDTA] pH 7.4). After a 3 min incubation step at RT, cells were centrifuged (300 x g, 10 min, RT) and washed once with phosphate buffered saline (PBS). Isolation yield ($5.83 \times 10^6 \pm$ 0.98) and cell viability ($92.08\% \pm 1.11$) were tested on a hemocytometer using the trypan blue exclusion assay.

BMC Transplant

Immediately after injury, 4×10^6 freshly isolated BMCs were resuspended in a final volume of 150 μL PBS (or vehicle) and injected through the lateral tail vein using a 30G needle. Number of transplanted cells was scaled down according to our results in rats (Piñero et al., 2018; Usach et al., 2017) and in results from the literature (Abreu et al., 2014).

Animals underwent functional tests and were euthanized at different survival times, after which sciatic nerves were dissected out. Experiments were then conducted on distal stumps and their results were compared to contralateral or sham nerves.

BMC Tracking. Exclusively for cell tracking experiments, BMCs were labeled with carboxyfluoresceinsuccinimidyl ester (CFSE) before transplantation as previously described by Bombeiro et al. (2016) and following the manufacturer's protocol. Briefly, 4×10^6 cells were incubated sheltered from light (20 min, 37°C) in 4 mL of a 5 nM CFSE solution prepared in PBS. The excess of fluorescent reagent was removed by a single wash with 20 mL PBS—10% FCS. Finally, the cells were resuspended in PBS for transplantation.

Functional Studies

Sciatic nerve functional recovery was evaluated through two different tests and, for each test, values were registered for the same animal at different survival times. Distal motor function was analyzed through an adapted walking test, and nociceptive function was evaluated as animal response to a hot stimulus.

Walking Test. Distal motor function was analyzed through an adapted walking test. Animals were placed inside an acrylic container (13 cm wide, 17 cm long, and 8 cm deep) placed on a glass base located 18 cm above a photographic camera. At least three photographs were taken in three different positions for each animal. The images obtained were processed with ImageJ software (NIH) to obtain the measures required for sciatic functional index (SFI) calculation following Baptista et al. (2007). The distances between the first and fifth finger (TS), the second and fourth finger (ITS), and the length of the footprint taken between the lower end and the tip of the third finger (PL) were calculated in both legs (I: ipsilateral, C: contralateral). The final value for each animal was obtained as the average of three images: $SFI = -38.3$ x $[(PL_I - PL_C)/PL_C] + 109.5$ x $[(TS_I - TS_C)/TS_C] + 13.3$ x $[(ITS_I - ITS_C)/ITS_C] - 8.8$.

Hot Plate Test. Nociceptive function was evaluated as animal response to a hot stimulus. Temperature was set at $52.5 \pm 0.02°C$ and the acrylic container described above was placed on top of the hot surface. Before surgery and at different survival times, the latency of the response was recorded as the number of seconds until each animal jumped or licked its hind paw. In the case of injured animals, the response time was recorded for both contralateral and ipsilateral legs, keeping latency time under 50 s to prevent damage by burning.

Myelin and Axonal Organization by Immunohistochemical Analysis

After sciatic nerve dissection at each survival time, nerves were fixed overnight in 4% paraformaldehyde (PFA)-PBS, pH 7.4, at 4°C. After fixation, PFA was replaced by 70% ethanol for at least 4 h at RT. Dehydration was continued by immersion in 96% ethanol (two 90 min steps, RT), absolute ethanol (two 30 min steps, RT), and xylol overnight at

4°C. Finally, sciatic nerves were embedded in paraffin and assembled in the corresponding supports. Longitudinal slices of 10 μm and cross-sections of 6 μm thickness were obtained using a microtome (RM2125 RTS, Leica) and mounted onto positively charged glass slides.

Before starting the immunostaining process, sections were rehydrated by immersion in xylene, ethanol (absolute, 96% and 70%, two 10 min steps each) and then washed twice with PBS. Antigen retrieval was carried out by heating sections at 90°C in 10 mM sodium citrate buffer, pH 6, containing 0.05% Tween 20 for 20 min.

For immunohistochemistry, sections were rinsed twice in PBS and three times in PBS-0.1% Triton X-100, and nonspecific protein binding sites were blocked with 5% FCS PBS-0.1% Triton X-100 (2 h, RT). Slides were then incubated overnight in a humid chamber at 4°C with primary antibodies (Table 2). After three washing steps in PBS-0.1% Triton X-100, samples were incubated with fluorophore-conjugated secondary antibodies (Table 2) plus 1 mg/mL 4′,6-diamidino-2-phenylindole for nuclei detection (2 h, RT). All antibodies were diluted in 1% FCS in PBS-0.1% Triton X-100. Finally, sections were rinsed three times in PBS-0.1% Triton X-100, five times in PBS and mounted with Mowiol antifading solution (10% in PBS, 50% glycerol, 200 mM Tris, pH 8.5). Controls were carried out by incubation without the primary antibodies. Images were taken using an Olympus BX100 epifluorescence microscope equipped with a CoolSnap digital camera and controlled by CellSens software.

Protein Detection in Sciatic Nerve Lysates

For protein analysis, sciatic nerve tissue was homogenized either in ice-cold TOTEX buffer (20 mM N-2-hydroxyethylpiperazine-N-2-ethane sulfonic acid [HEPES], pH 7.9, 350 mM NaCl, 1 mM $MgCl_2$, 0.5 mM EDTA, 0.1 mM ethylene glycol tetraacetic acid, 20% glycerol, 1% NP-40) for enzyme-linked immunosorbent assay (ELISA) or in ice-cold PBS supplemented with 1% NP-40 for cytokine quantification. Protease inhibitors were added to both buffers. Samples were centrifuged (11000 x *g*, 20 min, 4°C), the upper lipid phase was discarded, and the supernatant collected. Protein concentration was estimated by Bradford's assay. MBP levels were quantified by ELISA while cytokine quantification through a bead-based immunoassay.

Enzyme-Linked Immunosorbent Assay. Tissue lysates were diluted in PBS to a final protein concentration of 20 μg/mL, and 50 μL were seeded in a polystyrene high bind plate. All samples were analyzed by triplicate. After 2 h incubation at 37°C, nonspecific binding sites were blocked at 4°C with 3% nonfat dry milk in PBS-0.1% Tween-20. Samples were then incubated for 2 h with anti-MBP primary antibody and 2 more hours with the corresponding horseradish peroxidase-conjugated secondary antibody at RT in blocking solution

(Table 2). Three washes with PBS-0.1% Tween-20 were done in between incubation steps.

After Tween 20 removal through three washing steps with PBS, 0.03% H_2O_2 and 0.5 mg/mL o-phenylenediamine dihydrochloride (OPD) prepared in buffer citrate-phosphate 0.05 M, pH 5, were added to each well. Incubation was performed at RT and sheltered from light for 15 to 30 min. The reaction was stopped by the addition of 2.5 M H_2SO_4, and then absorbance was determined at 490 nm. Values were normalized to the control condition.

Cytokine Quantification. LEGENDplex™ Mix and Match System was used to quantify interleukin (IL)-1β (Cat. #740865), IL-6 (Cat. #740860), tumor necrosis factor (TNF) α (Cat. #740861), IL-10 (Cat. #740858), and free active transforming growth factor (TGF) $β_1$ (Cat. #740854). Distal stumps of injured sciatic nerves were homogenized as indicated above. Following the manufacturer's protocol, cytokines were immunolabeled and data were immediately acquired. Finally, cytokine concentration was calculated using LEGENDplex™ v8.0 software and normalized to the total protein values previously estimated by Bradford's assay.

Quantitative Polymerase Chain Reaction

Total RNA from distal stumps of sciatic nerves was obtained by combining two techniques. First, tissue was homogenized in Trizol™. Then the aqueous phase was transferred to RNA Clean & Concentrator-5 Spin-Columns in order to purify and concentrate the RNA. Finally, messenger RNA (mRNA) was reverse transcribed using Moloney murine leukemia virus reverse transcriptase, OligodT, and deoxynucleotide triphosphates. The reaction was carried out for 60 min at 42°C in a thermal cycler (Applied Biosystems).

Quantitative polymerase chain reaction (qPCR) assays were performed on a StepOnePlus™ thermal cycler (Applied Biosystems), employing MicroAmp 96-well plates and the SYBR Green Master Mix™PowerUp kit, in a final reaction volume of 10 μL. The general protocol used was as follows: activation (1 cycle: 50°C, 2 min), initial denaturation (1 cycle: 95°C, 2 min), amplification (40 cycles: 95°C, 3 s), and alignment-extension (1 cycle: 60°C, 30 s). At the end of each run, a dissociation curve was calculated to corroborate the amplification of a single product per well. IL-1β, IL-6, IL-10, TNFα, $TGFβ_1$ and arginase 1 (Arg-1) mRNA relative expression were calculated using glyceraldehyde 3-phosphate dehydrogenase as a housekeeping gene. Each sample was run in triplicate and statistical analysis was done using ΔCt values from three independent experiments. Primer-related data are listed in Table 3.

Flow Cytometry Analysis. Hidmark et al. (2017) protocol was followed for macrophage phenotype studies with slight modifications (Aranda et al., 2019). Each nerve, dissected and cut into small pieces, was placed in digestion medium consisting

Table 2. Antibodies Used in Immunohistochemistry and ELISA.

Antigen (conjugate)	Catalog number (brand)	Host (clonality)	Isotype (clone)	Dilution	
				IHC	ELISA
Primary antibodies					
bIII-tubulin	802001 (BioLegend)	Rabbit (polyclonal)	IgG	1:3000	
MBP	808402 (BioLegend)	Mouse (monoclonal)	IgG$_{2b}$ (SMI 99)	1:1000	1:2000
GAPDH	ab-8245 (Abcam)	Mouse (monoclonal)	IgG$_1$ (6C5)		1:5000
Secondary antibodies					
IgG rabbit (Alexa 488)	A21206 (Thermo Fisher)	Donkey (polyclonal)	IgG	1:500	
IgG mouse (Alexa 546)	A11030 (Thermo Fisher)	Goat (polyclonal)	IgG	1:500	
IgG mouse (HRP)	115-035-146 (Jackson ImmunoResearch)	Goat (polyclonal)	IgG		1:10000

Notes. ELISA: enzyme-linked immunosorbent assay; GAPDH: glyceraldehyde 3-phosphate dehydrogenase; HRP: horseradish peroxidase; IHC: immunohistochemistry; MBP: myelin basic protein.

of DMEM with 1.6 mg/mL collagenase IV and 10 µg/mL DNase I supplemented with 5 mM Mg^{2+}, 2.5 mM Ca^{2+} and 10 mM HEPES. Samples were incubated for 20 min at 37°C with shaking (450 rpm), and subsequently homogenized by pipetting up and down. The incubation-homogenization step was then repeated, and the enzymatic digestion process was stopped with 1 mM disodium EDTA prepared in PBS. Mechanical disaggregation was completed by passing the cell suspension through a 1mL syringe with a 25G needle. The final cell suspension was transferred to cytometer tubes.

Cell viability was tested by means of commercial reagent Zombie yellow following the manufacturer's protocol. At the end of incubation, and after washing with 5% FCS in PBS, nonspecific binding sites were blocked for 10 min at RT. The blocking solution was prepared with serum obtained from control mice, previously decomplemented for 30 min at 56°C with shaking (450 rpm) and diluted in a 1:2 ratio with 5% FCS in PBS-1 mM disodium EDTA (staining buffer).

After a washing step, cells were resuspended in staining buffer containing the corresponding primary antibodies, incubated for 20 min at 4°C in the dark and then washed with staining buffer. For fixation and permeabilization, cells were treated with 2% PFA in PBS supplemented with 1 mM disodium EDTA for 10 min at 4°C sheltered from light, and then treated with staining buffer supplemented with 0.25% saponin in identical conditions. Cells were then resuspended with the corresponding primary antibody diluted in staining buffer. After 30 min incubation at RT in the dark, saponin was removed by washing twice with staining buffer, and cells were resuspended in PBS-1 mM disodium EDTA. All centrifugation steps were carried out at 400 x *g* at 4°C. The details of the antibodies used are described in Table 4.

Flow cytometry analyses were conducted using a Becton-Dickinson FACSAriaII^{TM} cell analyzer (BD Biosciences). Unlabeled cells were used as autofluorescence control, and commercial beads as compensation controls following the protocol proposed by the manufacturer. The fluorescence minus one method was used to correctly delimit the populations.

Data analysis was performed using FlowJo v10.0.8 software (BD Biosciences). After doublet and nonviable cell exclusion, hematopoietic lineage cells were selected based on CD45 and CD11b expression and then macrophages were identified as F4/80$^+$, thus eliminating the remaining populations. Finally, the expression of CD86, CD206, major histocompatibility complex (MHC) II, inducible nitric oxide synthase (iNOS) and Arg-1 was analyzed in the population gated out.

Statistical Analysis. Statistical analysis was performed using GraphPad Prism (GraphPad Software). Statistical tests, post-tests, and significance values are indicated in the figure legends.

Results

Systemically Transplanted BMCs Migrate to the Lesion Nerve and Promote Axonal Regeneration and Remyelination

To initiate the assessment of the beneficial effects of transplanted BMCs on the demyelination–remyelination process, we first analyzed BMC migration to the lesion site. As shown in Figure 1a, CFSE-labeled BMCs were observed in

Table 3. Sequence of Primers Used for qPCR Analysis.

Gene	NCBI Ref sequence ID	Sequence	Product
Protein		Forward/reverse	
GAPDH	NM_001289726.1; NM_008084.3	5'-CCG TGT TCC TAC CCC CAA TG-3'	140 bp
Glyceraldehyde 3-phosphate dehydrogenase		5'-GGT CCT CAG TGT AGC CCA AG-3'	
IL-1β	NM_008361.4	5'-GCA ACT GTT CCT GAA CTC AAC T-3'	89 bp
Interleukin 1, beta		5'-ATC TTT TGG GGT CCG TCA ACT-3'	
TNFα	NM_013693.3; NM_001278601.1	5'-AGC AAA CCA CCA AGT GGA GGA-3'	105 bp
Tumor necrosis factor alpha		5'-GCT GGC ACC ACT AGT TGG TTG T-3'	
IL-6	NM_031168.2	5'-TAG TCC TTC CTA CCC CAA TTT CC-3'	76 bp
Interleukin 6		5'-TTG GTC CTT AGC CAC TCC TTC-3'	
IL-10	NM_010548.2	5'-ACA GCC GGG AAG ACA ATA AC-3'	116 bp
Interleukin 10		5'-CAG CTG GTC CTT TGT TTG AAA G-3'	
TGFβ1	NM_011577.2	5'-ACG TCA CTG GAG TTG TAC GG-3'	131 bp
Transforming growth factor, beta 1		5'-TTT GGG GCT GAT CCC GTT G-3'	
Arg-1	NM_007482.3	5'-TGG CTT GCG AGA CGT AGA C-3'	160 bp
Arginase 1		5'-GCT CAG GTG AAT CGG CCT TTT-3'	

Notes. bp: base pairs; GAPDH: glyceraldehyde 3-phosphate dehydrogenase; NCBI: National Center for Biotechnology Information; qPCR: quantitative polymerase chain reaction.

the crush area as soon as 3 days postinjury (dpi) and still detected 7 and 14 dpi (Supplemental Figure 1).

We next analyzed the effect of transplanted cells on remyelination by quantifying MBP through ELISA in distal nerve segments. While MBP levels remained high and comparable to noninjured nerves 1 dpi, a marked decrease—which was sharper in BMC-transplanted animals—was observed 3 dpi. By 7 dpi, MBP levels seemed to reach a minimum in both experimental groups. As from 10 dpi, however, BMCs were able to promote faster sciatic nerve remyelination (Figure 1b), with a stronger recovery and significantly higher MBP levels in treated than in non-treated animals at 14 dpi.

As a complementary approach, cross-sections of the lesion area at different survival times were submitted to MBP and bIII-tubulin immunodetection as markers of axons and myelin, respectively (Figure 2). At 3 dpi, zones devoid of MBP staining, indicative of the onset of demyelination, were detected in both transplanted and non-transplanted animals (Figure 2). Areas where structures were still compatible with myelinated axons mostly showed the absence of bIII-tubulin expression, a sign of axonal degeneration. Worth highlighting, an overlap between MBP and bIII-tubulin marker immunoreactivity was observed in the distal stump of both experimental groups (digital magnification, arrowheads), which shows a loss of myelin integrity in myelinated axons. By 7 dpi (Figure 2), demyelination became more evident with the presence of classic ovoid bodies commonly known as clusters (digital magnification, solid arrows). At 10 dpi, myelin remnant removal was almost complete in both experimental groups and early signs of remyelination were detected in some axons of treated animals (digital magnification, hollow arrows). bIII-tubulin immunodetection also indicated that regeneration

was underway. Finally, by 14 dpi ongoing remyelination was found in both treated and non-treated animals by 14 dpi. Even though an apparent higher number of myelinated axons was observed in treated animals (64.68 ± 7.118 axons/field), no significant differences was found when compared with non-treated animals (57.27 ± 7.974 axons/field, *p* value: .29).

Functional Recovery is Fostered by Systemically Transplanted BMC

Since axonal regeneration and remyelination are not always followed by functional recovery, walking track and hot plate tests were performed to determine functional parameters. As early as 1 dpi, animals of both experimental groups suffered a close-up between fingers and a reduction in footprint length (Figure 3a), which were reflected by a decrease in the distances measured and, consequently, in the SFI (Figure 3b). A slight extension between the first and fifth fingers was observed as from 3 dpi, while an increase in the distance between the second and fourth fingers and the lengthening of the footprint were observed by 7 dpi. In sum (Figure 3b), an abrupt drop was established in SFI values 1 dpi, which tended to recover until reaching control values 2 weeks after surgery in both groups. Of note, BMC-transplanted animals recovered faster, showing significantly higher SFI values than those of non-treated animals 1, 3, and 7 dpi.

In addition to SFI recovery after injury, hot plate test results showed benefits in terms of nociceptive function. Results showed a loss in ipsilateral nerve sensitivity as a consequence of injury, as lesioned animals were unable to respond to hot stimuli from the first day (Figure 3c). As from 10 dpi, recovery became apparent in both groups, with non-treated animals slowly regaining sensitivity and, most

Table 4. Antibodies Used in Flow Cytometry.

Antigen (fluorophore)	Catalog number (brand)	Host (clonality)	Isotype (clone)	Dilution
Extracellular antigens				
CD11b (PerCP)	101229 (BioLegend)	Rat (monoclonal)	$IgG_{2b, k}$ (M1/70)	1:80
CD45 (APC-Fire750)	103153 (BioLegend)	Rat (monoclonal)	$IgG_{2b, k}$ (30-F11)	1:80
F4/80 (BV711)	123147 (BioLegend)	Rat (monoclonal)	$IgG_{2a, k}$ (BM8)	1:80
MHC II (SB436)	63-5321-80 (Thermo Fisher)	Rat (monoclonal)	$IgG_{2a, k}$ (M5/114.15.2)	1:125
CD86 (PE-Cy7)	105014 (BioLegend)	Rat (monoclonal)	IgG_{2a} (GL-1)	1:20
CD206 (APC)	141708 (BioLegend)	Rat (monoclonal)	$IgG_{2a, k}$ (C068C2)	1:40
Intracellular antigens				
iNOS (PE)	12-5920-80 (Thermo Fisher)	Rat (monoclonal)	$IgG_{2a, k}$ (CXNFT)	1:250
Arginase-1 (Alexa 488)	53-3697-80 (Thermo Fisher)	Rat (monoclonal)	$IgG_{2a, k}$ (AlexF5)	1:50

important, BMC-transplanted animals exhibiting significantly shorter latency and earlier normalization. Contralateral nerve latency, evaluated as an internal control, remained unaltered at all survival times along the experiment in both groups.

BMCs Modulate the Injury-Associated Immune Response

The degeneration promoted by sciatic nerve compression gives way to an inflammatory response in which repairing SCs are initially responsible for producing pro-inflammatory cytokines (Jessen & Arthur-Farraj, 2019; Jessen & Mirsky, 2016). As an initial study of the potential modulatory effects of BMCs on the lesion-associated inflammatory response, mRNA expression of classical cytokines and enzymes involved in this process was quantified through qPCR.

As expected, due to the inflicted injury, expression of IL-1β, IL-6, and TNFα was detected in both experimental groups as soon as 4 h after lesion. Transplanted BMCs recruited into the lesion area promoted a significant decrease of these three cytokines 3 dpi (Figure 4a–c). However, at 7 dpi, treated animals showed a new increase in IL-1β and TNFα mRNA and, though not significant, in IL-6 mRNA. The anti-inflammatory cytokine par excellence, IL-10 showed a significant increase in BMC-transplanted animals 1, 3, and 7 (Figure 4d), while TGFβ₁ was only found significantly upregulated 3 dpi (Figure 4e). We also determined the mRNA levels of one of the enzymes classically associated with macrophage phenotypes, Arg-1. Arg-1 mRNA was significantly upregulated 3 and 7 dpi (Figure 4f).

On the basis of qPCR results, we next determined cytokine concentration in the distal stumps of lesioned nerves. As shown in Figure 5a and b, treated animals showed a decreased production of pro-inflammatory cytokines IL-1β and TNFα only at 3 dpi, but no significant differences in IL-6 synthesis were observed (Figure 5c). In turn, an increase in IL-10 production due to BMC transplant was detected 3 and 7 dpi (Figure 5d), while free active TGFβ₁ was upregulated only 1 week after treatment (Figure 5e).

The downregulation of pro-inflammatory cytokines 3 dpi, the upregulation of IL-10, and the well-known role of nerve-associated macrophages in the orchestration of the inflammatory response after injury, motivated a detailed study of their phenotypic shifts. Although no significant differences in the expression of CD86 (Figure 6b) or MHC II (Figure 6c), BMC transplantation promoted a decrease in the proportion of iNOS⁺ macrophages throughout the survival times studied (Figure 6d). Treated animals also showed a significantly higher percentage of CD206⁺ cells at 3, 10, and 14 dpi (Figure 6e) and a substantially increased proportion of Arg-1⁺ macrophages, specifically at 3 dpi (Figure 6f). However, an inversion of these values was observed at 7 dpi. Finally, Arg-1⁺ cells reached equal levels in both groups toward 10 and 14 dpi. Worth highlighting, the analysis of CD45 versus CD11b dot plots revealed a sustained increase in the CD45⁺CD11b⁻ population throughout the four survival times studied. Notably, treated animals showed higher levels of CD45⁺CD11b⁻ cells by 10 dpi (Figure 6g).

Discussion

The sciatic nerve compression model is widely used for the study of reversible WD and constitutes an attractive tool to try out potential treatments for nervous system damage
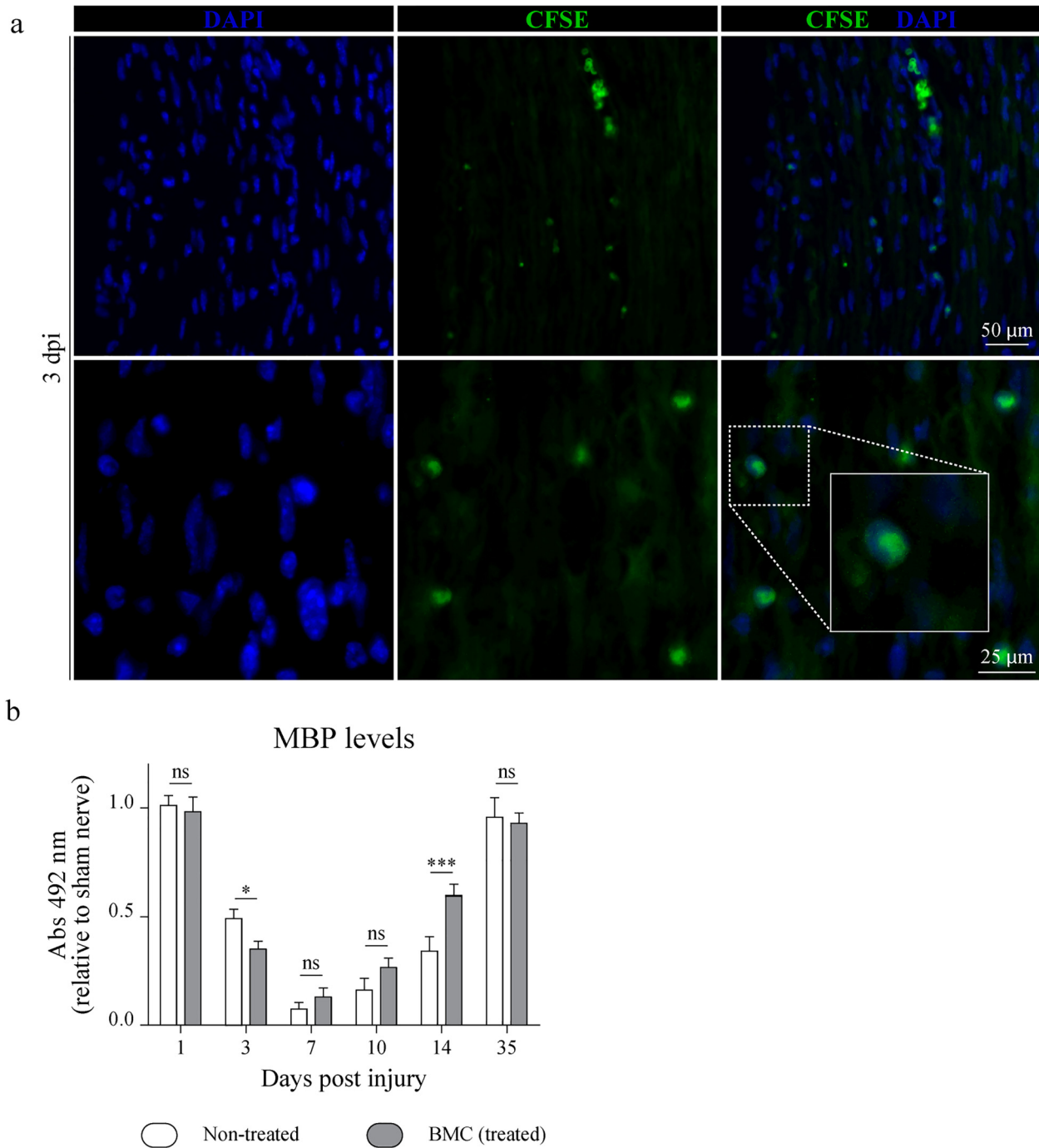
Figure 1. Migration of transplanted CFSE⁺-BMCs to the lesion area and effect of BMC transplant on MBP levels. (a) BMCs were labeled with CFSE prior to transplant and animals were then sacrificed 3, 7, and 14 dpi (7 and 14 dpi are shown in Supplemental Figure 1). Representative epifluorescence microscopy images obtained from longitudinal sections of the lesion area (40x and 100x). CFSE⁺ cells (green) and nuclei counterstained with DAPI (blue). Insets in merged images show digital amplifications of areas in dotted line boxes. (b) Immunodetection of MBP through ELISA in homogenates of sham nerves and distal areas of ipsilateral nerves of non-treated (white) or BMC-transplanted animals (gray), 1, 3, 7, 10, 14, and 35 dpi. Absorbance values (492 nm) obtained in three independent experiments (one animal per experimental group) were normalized to the sham nerve and are expressed as the mean ± SD. Statistical analysis performed through two-way ANOVA (p value for interacting significance: .0003), followed by Bonferroni's multiple comparison post-test (* $p < .05$; ** $p < .01$; *** $p < .001$). ANOVA: analysis of variance; BMC: bone marrow cell; CFSE: carboxyfluoresceinsuccinimidyl ester; DAPI: 4′,6-diamidino-2-phenylindole; ELISA: enzyme-linked immunosorbent assay; MBP: myelin basic protein; ns: not significant; SD: standard deviation.
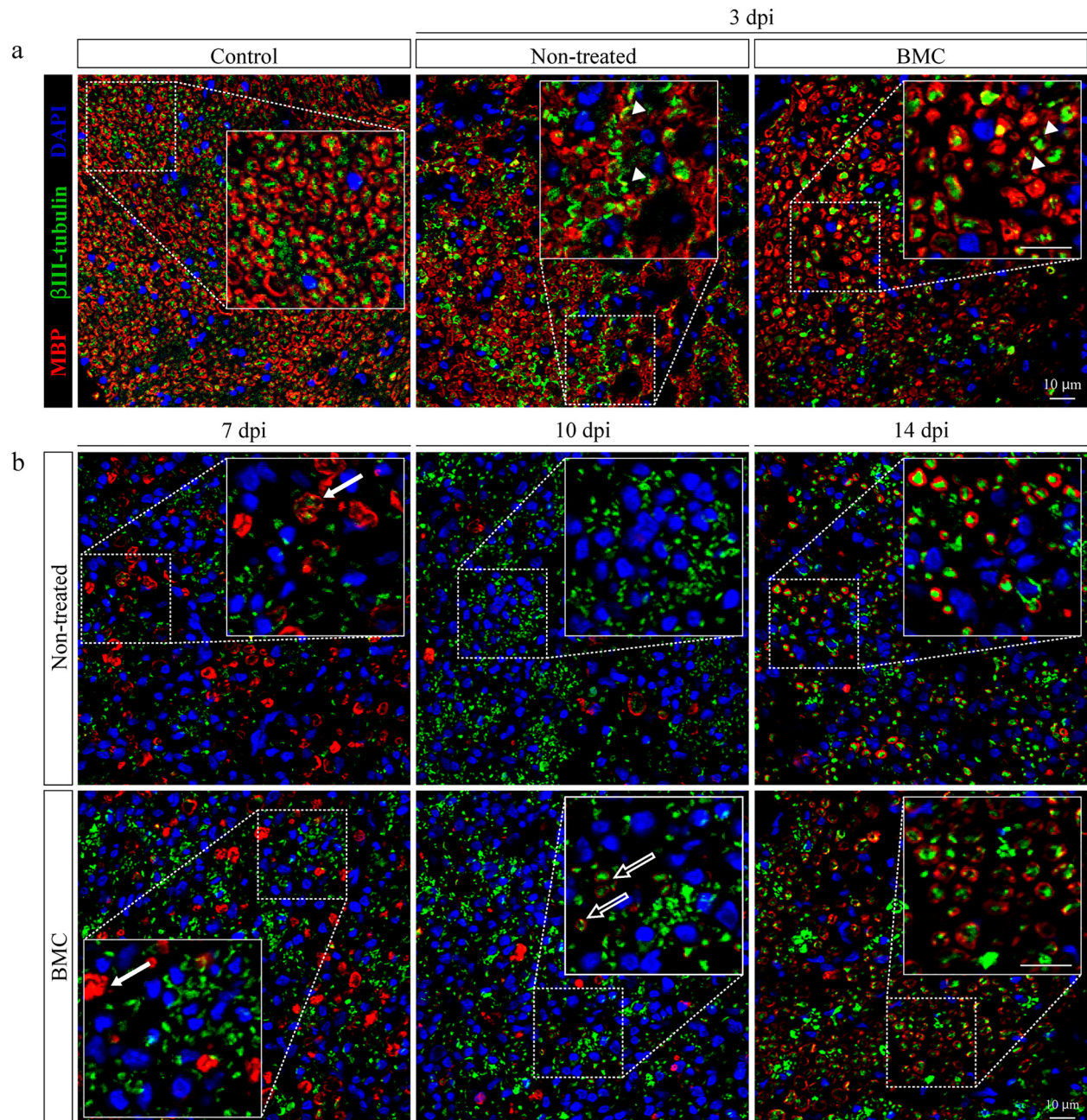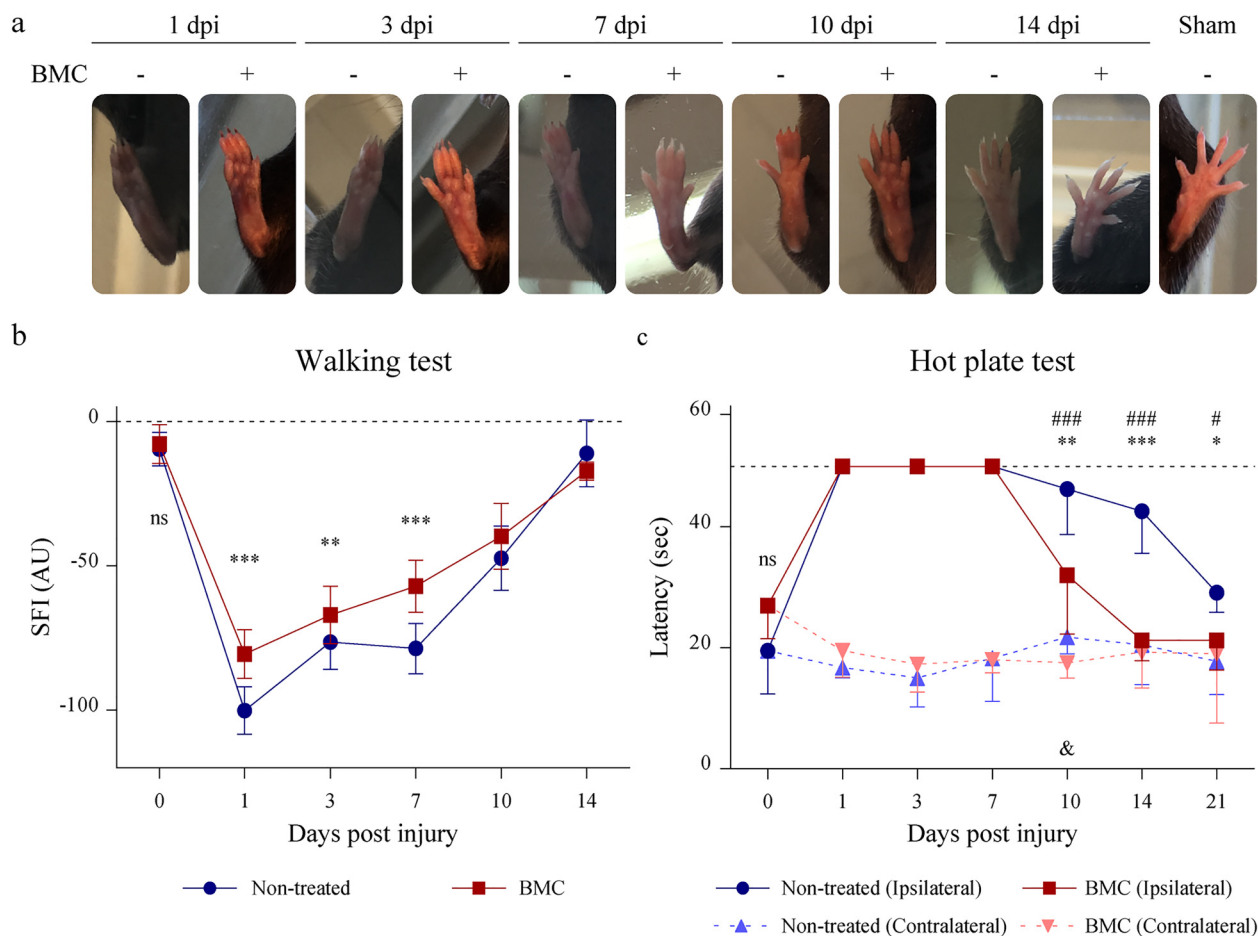
Figure 2. Effect of BMC transplant on bIII-tubulin and MBP organization. Immunofluorescence detection of axonal marker bIII-tubulin (green) and myelinating SC MBP (red), nuclei counterstained with DAPI (blue) in cross-sections of control nerves and distal areas of ipsilateral nerves of non-treated and BMC-transplanted animals (a) 3 dpi and (b) 7, 10, and 14 dpi. Representative images obtained by confocal microscopy (40x). The bIII-tubulin and MBP immunostaining overlap (arrowheads), ovoid bodies (solid arrows), and incipient remyelinated axons (hollow arrows) are shown as digital amplifications of areas in dotted line boxes. BMC: bone marrow cell; DAPI: 4′,6-diamidino-2-phenylindole; MBP: myelin basic protein; SC: Schwann cell.

(Geuna, 2015; Savastano et al., 2014; Sta et al., 2014). The results presented in this manuscript show that systemically transplanted mice BMCs preserve the beneficial effects of their rat counterparts in migrating to the lesioned area, promoting remyelination, and accelerating functional recovery in the damaged nerve.

The recruitment of transplanted cells in injured tissues has been widely described (Bittira et al., n.d.; Bell et al., 2011; Kavanagh & Kalia, 2011) and also assessed by our group (Piñero et al., 2018; Setton-Avruj et al., 2007; Soto et al., 2021; Usach et al., 2017). The evaluation of BMC recruitment until 60 days postinjury to other organs demonstrated no

Figure 3. Effect of BMC transplant on functional parameters. (a) Representative photographs used to determine parameters required for SFI calculations. (b) Graphs summarizing values obtained for (b) SFI and (c) response time to hot stimulus. In both cases tests were performed on the same animal throughout survival times. Values were obtained in four independent experiments (one animal per experimental group) and are expressed as the mean ± SD. Statistical analysis performed through repeated measures two-way ANOVA (p value for interacting significance: SFI, < .0001; and response time to hot stimulus, < .0001), followed by Bonferroni's multiple comparison post-test. Significance: * differences between ipsilateral legs of non-treated animals and BMC-transplanted animals; # differences between the ipsilateral and contralateral leg of non-treated animals; & differences between the ipsilateral and contralateral leg of BMC-transplanted animals (*/#/& p < .05; **/##/&& p < .01; ***/###/&&& p < .001). ANOVA: analysis of variance; BMC: bone marrow cell; ns: not significant; SFI: sciatic functional index.

presence of labeled cells even in the contralateral sciatic nerve. However, we cannot discard the migration of transplanted multipotent cells to other organs in our experimental model.

In non-treated animals, MBP levels along WD were comparable to those reported previously (Piñero et al., 2018; Soto et al., 2021; Usach et al., 2011, 2017) and in keeping with results recently obtained using single-cell RNA sequencing technology (Brosius Lutz et al., 2022). Functionally, our SFI values agreed with those observed in similar injury models (Baptista et al., 2007; Bombeiro et al., 2016, 2018; Hsieh et al., 2017; Peluffo et al., 2015). Moreover, areas co-expressing bIII-tubulin and MBP immunostaining at 3 dpi are in line with a recent report by Catenaccio et al. (2017), who describe the relationship between ovoid body

formation and axonal fragmentation, a process carried out by SCs shortly after injury . The results of the present manuscript clearly demonstrate that myelin breakdown is exacerbated in treated animals at 3 days postinjury. However, the recovery, although not significant until 14 days postinjury, was accelerated in the treated group (Figure 1), suggesting that BMC transplant may accelerate myelin debris removal bringing about a faster remyelination, as previously demonstrated by our group and bibliographic data showing that myelin debris removal is an essential step for remyelination and axonal regeneration promoting behavioral and functional recovery (Schäfer et al., 1996; Shen et al., 1998; Usach et al., 2017).

The integrated analysis of remyelination and functional recovery revealed a temporal discrepancy, as the latency
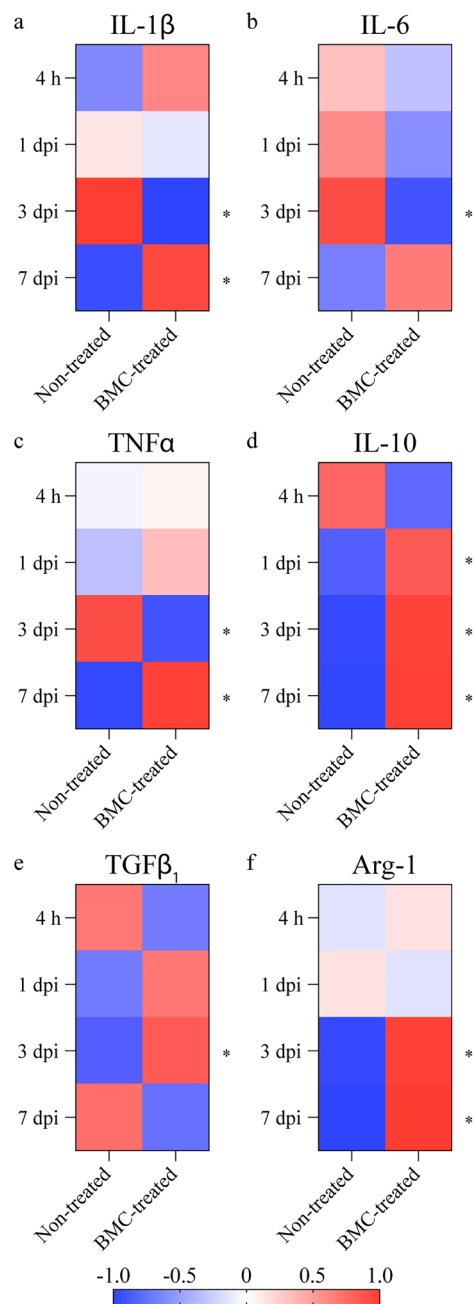
Figure 4. Gene expression of cytokines involved in the lesion-associated inflammatory process. Relative quantification of mRNA expression of (a) IL-1β, (b) TNFα, (c) IL-6, (d) IL-10, (e) TGFβ₁, and (f) Arg-1. qPCRs were performed using cDNA synthesized from mRNA isolated from distal areas of injured sciatic nerves of non-treated and BMC-transplanted animals. GAPDH was used as a housekeeping gene. Heat maps represent Z-score values of data obtained in three independent experiments (one animal per experimental group). Statistical analysis performed through Student t-test comparing treated and non-treated animals within each survival time (* $p < .05$). Arg-1: arginase 1; BMC: bone marrow cell; cDNA: complementary DNA; GAPDH: glyceraldehyde 3-phosphate dehydrogenase; IL: interleukin; mRNA: messenger RNA; ns: not significant; qPCR: quantitative polymerase chain reaction; TGF: transforming growth factor; TNF: tumor necrosis factor.
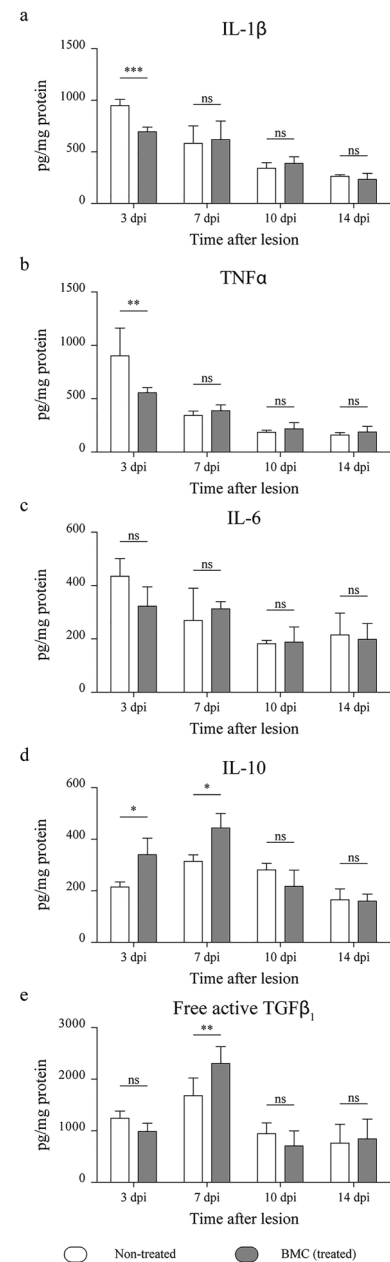
Figure 5. Quantification of pro-inflammatory and anti-inflammatory cytokines. Cytokine quantification performed on protein lysates obtained from distal stumps of injured sciatic nerves of non-treated (white box) and BMC-transplanted animals (gray box) through a bead-based immunoassay. Concentration of (a) IL-1β, (b) TNFα, (c) IL-6, (d) IL-10, and (e) free active form of TGFβ₁ relativized to total protein in each sample previously estimated by Bradford's assay. Values were obtained in three independent experiments (one animal per experimental group) and are expressed as the mean ± SD. Statistical analysis performed through two-way ANOVA(p value for interacting significance: IL-1β, .0002; TNFα, .0124; IL-6, .3335; IL-10, .0044; and free active form of TGFβ₁, .0026), followed by Bonferroni's multiple comparison post-test (* $p < .05$; ** $p < .01$; *** $p < .001$). ANOVA: analysis of variance; BMC: bone marrow cell; IL: interleukin; ns: not significant; TGF: transforming growth factor; TNF: tumor necrosis factor; SD: standard deviation.
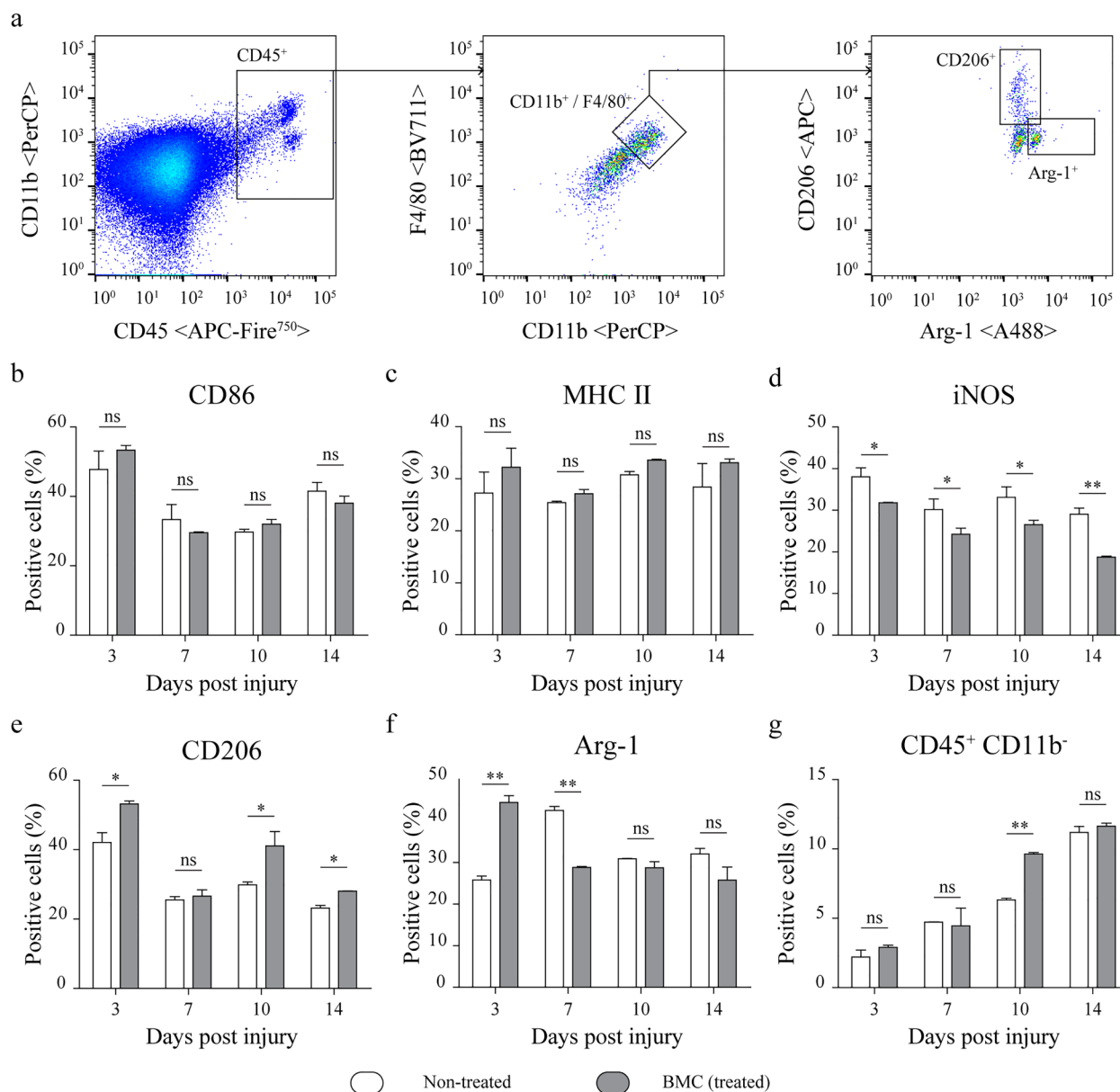
Figure 6. Lesion-associated macrophage phenotypes. Flow cytometry analysis of phenotype-specific macrophage markers performed on cell suspensions obtained by mechanical and enzymatic digestion of the distal portions of sciatic nerves dissected from non-treated (white) and BMC-transplanted animals (gray). (a) Representative graphs of the gating strategy used to select the CD45 $^+$ CD11b $^+$ F4/80 $^+$ population and analysis of macrophage markers (b) CD86, (c) MHC II, (d)iNOS, (e) CD206 and (f) Arg-1. (g) Proportion of CD45 $^+$ CD11b $^-$ cells. Bar graphs summarize values obtained in four independent experiments (one animal per experimental group) and expressed as the mean ± SD. Statistical analysis performed through two-way ANOVA (p value for interacting significance: CD86, .1110; MHC II, .7775; iNOS, .3055; CD206, .0166; Arg-1, < .001; and CD45 $^+$ CD11b $^-$ .0046), followed by Bonferroni's multiple comparison post-test (* $p < .05$; ** $p < .01$). ANOVA: analysis of variance; Arg-1: arginase 1; BMC: bone marrow cell; iNOS: inducible nitric oxide synthase; MHC: major histocompatibility complex; ns: not significant; SD: standard deviation.

upon hot stimulus normalized before MBP levels. This difference may respond to the fact that, on the one hand, the hot plate test analyzes nerve impulse originated in high-temperature-sensing thermoreceptors (> 52 °C) and transmitted through Aδ type fibers (Dhaka et al., 2006); on the other hand, MBP assessment through ELISA implies the quantification of protein levels in the whole distal stump, including the highly myelinated axons. For these reasons, we hypothesize that the improvement observed in sensory function is associated with small-caliber axons wrapped by a thinner myelin sheath and undergoing earlier remyelination, which will not necessarily be reflected in overall MBP levels. Images obtained

at the site of injury showing early remyelinated axons may support this hypothesis. Also, this result is in agreement with previous findings showing that systemically transplanted bone marrow mononuclear cells prevent neuropathic pain, even upon complete demyelination (Usach et al., 2017).

It is important to understand why the experiments included in the manuscript were performed only in males, bibliographical data support our decision. One of the main problems associated with peripheral nerve injuries is the persistent neuropathic pain, usually resistant to actual treatments. These treatments usually include nonaddictive analgesic strategies, often centered on neuroimmune modulation (Myers & Shubayev, 2011; Scholz & Woolf, 2007). Recently have been demonstrate a marked female predominance in pain (Bouhassira et al., 2008; Fillingim et al., 2009), although they are underrepresented in preclinical (Mogil et al., 2000) and basic research, as only male subjects are used. This may be explained by the assumption that estrous cyclicity introduces additional variability.

It has been demonstrated sexual dimorphism in rodent DRG transcriptomes in response to peripheral nerve injury (Ahlström et al., 2021; Stephens et al., 2018), hyperalgesic priming by IL-6 (Paige et al., 2020), sciatic nerve injection of MBP derived peptides (Chernov et al., 2020), and other stimuli.

In terms of neuropathic pain, microglia-neuronal signaling pathway is relevant only to male mice (Mapplebeck et al., 2015); also, they exhibited upregulation of chemokines, stimulation of neuroinflammation signaling, and toll-like receptor signaling (Miller et al., 2020; Ramachandran et al., 2019; Stokes et al., 2013). A reduction of mRNAs encoding calcium, sodium, and potassium ion channels as well as ionotropic α-amino-3-hydroxy-5-methyl-4-isoxazolepropionic acid (AMPA), N-methyl-D-aspartate (NMDA), and gamma aminobutyric acid (GABA) receptors (Chernov & Shubayev, 2021) occurred also in male animals.

In females, prostaglandin signaling and neuroendocrine mechanisms involving prolactin receptors (Chernov et al., 2020; Mecklenburg et al., 2020; North et al., 2019; Paige et al., 2020; Ray et al., 2019) are involved in hypersensitivity; also, IL-17a participate in mechanical hypersensitivity (Luo et al., 2021). In females, a relevant role of MBP peptides in pain was observed, with the pro-allodynic MBP (84–104) fragment present in female mice (Lee et al., 2022). If MBP proteolysis is inhibited, mechano-allodynia was attenuated in part by blocking the release of T-cell epitopes of MBP and T-cell homing into the nerve (Hong et al., 2017; Kobayashi et al., 2008; Liu et al., 2012).

The intricate interplay of cytokines involved in the inflammatory response associated with WD makes their study particularly complex. To determine whether the effect of transplanted cells is in part mediated by an immunomodulatory mechanism, we drew on gene and protein quantification through qPCR and a bead-based immunoassay, respectively. In general terms, the changes observed in cytokine mRNA

expression in non-transplanted animals were consistent with those described in the literature (Büttner et al., 2018; Nadeau et al., 2011; Peluffo et al., 2015; Rotshenker, 2011; Ydens et al., 2012). Regarding cell therapy and in spite of diverse effects, BMC transplant promoted a decrease in the expression of proinflammatory cytokines IL-1β and TNFα specifically at 3 dpi. Even if a proinflammatory environment is often considered harmful, certain proinflammatory cytokines aid peripheral regeneration by participating in the recruitment and activation of immune cells, which in turn leads to myelin debris removal and SC activation and differentiation, both essentials stages for remyelination and axonal regeneration (Bastien & Lacroix, 2014; Jessen & Mirsky, 2016; Klein & Martini, 2016; Lutz et al., 2017; Nadeau et al., 2011; Perrin et al., 2005). It should be noted that the attenuation of pro-inflammatory cytokines did not affect nerve regeneration or functional recovery. Also, an upregulation was detected in IL-10 mRNA over the first week after treatment and in protein quantity 3 and 7 dpi. In particular, this may be considered a promising result, given that IL-10 has been proven essential in the resolution of inflammation, a crucial step in nerve regeneration (Mietto et al., 2015). Finally, an increase in TGFβ free active form was detected at 7 dpi. TGFβ is upregulated after nerve lesion in SCs, fibroblasts and also macrophages (Jessen & Arthur-Farraj, 2019); even though TGFβ signaling is involved in controlling both proliferation and apoptosis in developing nerves (D'Antonio et al., 2006), it is also a key mediator of peripheral nerve regeneration after injury (Clements et al., 2017) and plays a protective role against injury-induced neuropathic pain (Lantero et al., 2012). Worth pointing out, the survival times where these effects were observed coincide with the influx and permanence of hematogenous macrophages and transplanted cells. In sum, gene expression results suggest BMC involvement in the modulation of the inflammatory environment associated with WD.

Ample evidence supports a powerful immunomodulatory effect of mesenchymal stem cells derived from compartments such as the bone marrow or adipose tissue (Caplan & Sorrell, 2015; Catenaccio et al., 2017; Rilo et al., 2017; Marinescu et al., 2021; Qu et al., 2018; Savastano et al., 2014) on peripheral and central nervous system injuries (Aurora & Olson, 2014; Brini et al., 2017; Evangelista et al., 2018; Huh et al., 2017; Takahashi et al., 2018; Zhang et al., 2013). Accordingly, the changes observed in lesion-associated cytokine profiles after BMC administration in different experimental models (Abreu et al., 2014; Brenneman et al., 2010; Leal et al., 2014) could be at least partially attributed to the small fraction of mesenchymal stem cells present in the suspension after bone marrow extrusion. Indeed, Kalinski et al. (2020) have shown that mesenchymal progenitor cells migrate to the injured nerve and shape the immune milieu, supporting both previous (Usach et al., 2011) and current findings.

Over 20 years ago, Mills et al. introduced classification of macrophages into M1 and M2 (Macrophages et al., 2000).

Since then, technological advances promoted the improvement of cell marker detection and most importantly their transcriptome, making the study of the phagocytes par excellence evolve to the concept of a wide spectrum of macrophages phenotypes. Nevertheless, M1/M2 is still the simplest starting point (Mills, 2012).The main differentiation is based on the arginine metabolism (Rath et al., 2014). M1 macrophages produce nitric oxide (NO) through the activity of iNOS, leading to the release of reactive nitrogen species normally associated with cell damage. On the other hand, M2 macrophages express Arg-1, consuming arginine without NO synthesis and generating important metabolites for tissue repair. In this context, we used multiparameter flow cytometry to study markers commonly associated with M1 and M2 macrophage phenotypes at the site of injury and obtained findings which are in keeping with previous reports. Briefly, even though M1 is the main representative phenotype found at the beginning of the inflammatory response (Nadeau et al., 2011), some of the genes with the highest induction 1 dpi are, in fact, those encoding for anti-inflammatory markers such as β-N-acetylhexosaminidase (YM1), Arg-1, and CD206 (DeFrancesco-Lisowitz et al., 2015; Stratton et al., 2018). The initial pro-inflammatory response gradually gives way to a transition from M1 to M2, which prevails after the third day (Mietto et al., 2015; Nadeau et al., 2011). In addition to the sustained decrease in iNOS$^+$ macrophages throughout the time points analyzed, BMC transplant induced a significantly higher relative number of Arg-1$^+$ and CD206$^+$ cells 3 dpi. These results agree with those obtained through qPCR and bead-based immunoassays, such as the attenuation of pro-inflammatory mediators and an increase in anti-inflammatory cytokines. The immunomodulatory action as well as the change in macrophage phenotype promoted by BMC in the present experimental model could be reproduced in other degenerative processes or pathological scenarios whose pathophysiology involves pro-inflammatory macrophages.

Even though macrophages are known to be critical for nerve regeneration and remyelination (Niemi et al., 2013; Stratton et al., 2018; Zigmond & Echevarria, 2019), the role of their wide range of phenotypes and their complex cytokine profile in the context of sciatic nerve lesion is less clear and somewhat controversial. Recent studies have classified lesion-associated phagocytes in a continuum of eight clusters and shown them to adapt phenotypes to the different microenvironmental conditions found along the regenerating nerve (Canè et al., 2019; Kalinski et al., 2020). *In vitro* experiments show that exposure to M1 macrophage-conditioned media reduces SC proliferation, while M2 macrophage-conditioned (Mokarram et al., 2012) and macrophage-derived microvesicle media (Zhan et al., 2015) enhance SC migration and proliferation and promote axonal growth. Moreover, an *in vivo* study with perineural-transplanted M2 macrophages generated *in vitro* has evidenced a reduction in neuropathic pain mediated by the release of opioid peptides (Pannell et al.,

2016). Additionally, M1 macrophages have proven to be essential for efficient regeneration, while a sharp shift into M2 has been shown to actually hinder axonal growth and behavioral outcomes (Peluffo et al., 2015). Thus, striking a balanced microenvironment might be essential for any approach aiming at nerve regeneration and the attenuation of neuropathic pain.

The timely modulation of the immune response has proven beneficial to recovery after not only peripheral nerve lesion (Mokarram et al., 2017) but also spinal cord injury (Kigerl et al., 2009; Kobashi et al., 2020; Kroner et al., 2014; Park et al., 2019). In our experimental model, an early-onset phenotype change was observed as a result of BMC transplant, which might partly explain the effects of cell therapy. However, the interaction with other cell types like the CD45$^+$CD11b$^-$ population still needs to be determined, as they have been strongly associated with the inflammation process and nerve function recovery (Bombeiro et al., 2016, 2020). Thus, new studies are required to elucidate the link between the positive impact of transplanted cells on remyelination and pain relief and the modulation of the immune microenvironment.

Despite the complexity of the inflammatory process in WD, reflected by the elaborate network of interactions among SCs, fibroblasts and macrophages, the current results further show the recruitment of transplanted BMCs and their ability to help nerve regeneration.

It is worth mentioning that BMC initial effect resides in accelerating myelin debris removal and modulating the inflammatory response associated with the lesion, which is reflected by an accelerated long-term recovery. Thus, the immunomodulatory effect of BMC is exerted at the first days after the injury while after 7 days postinjury they play their beneficial effect contributing to myelin debris removal and at latest survival times they transdifferentiate to SCs (Piñero et al., 2018). In parallel, BMC may affect the degenerative microenvironment of the injured nerve which may be reflected by changes in the macrophages phenotype later on. To sum up, BMC easy isolation without the need for *in vitro* expansion, the negligibly low risks associated with unwanted phenotypic changes and low immunogenicity, the possibility of noninvasive administration, the long-established benefits in morphological and functional recovery and the newly described immunomodulatory capacity reinforce BMC autologous transplant as a promising therapeutic option for peripheral nervous system injuries.

Author's Notes

Gonzalo Piñero, Marianela Vence, Magalí C. Cercato, Paula A. Soto, Vanina Usach and Patricia C. Setton-Avruj are also affiliated with Department of Pathology, Molecular & Cell-Based Medicine, Mount Sinai Hospital, New York, NY, USA.

Availability of Data and Material

Data supporting these findings are available on reasonable request.

Ethics Approval

All animals used in this study were treated humanely and all procedures were performed in accordance with the guidelines of the Committee of Bioethics at Facultad de Farmacia y Bioquímica, Universidad de Buenos Aires (CICUAL-FFyB; Exp. 68987/2017; Res. CD2651/2018) and following the NIH Guide for the Care and Use of Laboratory Animals and EU Directive 2010/63/EU for animal experiments of the European Commission. Eight-week-old to 10-week-old C57BL/6J mice were housed in standard cages in a temperature-controlled room ($22°C \pm 2°C$) on a 12 h light-dark cycle. Food and water were provided *ad libitum*.

Authors' Contributions

GP and PS-A designed the study and wrote the manuscript. GP, MV, MLA, MCC, PAS, and VU performed the experiments. GP and PS-A analyzed and interpreted data. PS-A secured funding for the study. All authors read and approved the final manuscript.

Declaration of Conflicting Interests

The authors declared no potential conflicts of interest with respect to the research, authorship, and/or publication of this article.

ORCID iD

Patricia C. Setton-Avruj https://orcid.org/0000-0002-4094-7712

Supplemental Material

Supplemental material for this article is available online.

References

Abreu, S. C., Antunes, M. A., Mendonça, L., Branco, V. C., De Melo, E. B., Olsen, P. C., Diaz, B. L., Weiss, D. J., Paredes, B. D., Xisto, D. G., Morales, M. M., & Rocco, P. R. M. (2014). Effects of bone marrow mononuclear cells from healthy or ovalbumin-induced lung inflammation donors on recipient allergic asthma mice. *Stem Cell Research & Therapy*, *5*, 108–119. https://doi.org/10.1186/scrt496

Ahlström, F. H. G., Mätlik, K., Viisanen, H., Blomqvist, K. J., Liu, X., Lilius, T. O., Sidorova, Y., Kalso, E. A., & Rauhala, P. V. (2021). Spared nerve injury causes sexually dimorphic mechanical allodynia and differential gene expression in spinal cords and dorsal root ganglia in rats. *Molecular Neurobiology*, *58*, 5396–5419. https://doi.org/10.1007/s12035-021-02447-1

Aranda, M. L., Guerrieri, D., Piñero, G., González Fleitas, M. F., Altschuler, F., Dieguez, H. H., Keller Sarmiento, M. I., Chianelli, M. S., Sande, P. H., Dorfman, D., & Rosenstein, R. E. (2019). Critical role of monocyte recruitment in optic nerve damage induced by experimental optic neuritis. *Molecular Neurobiology*, *56*, 7458–7472. https://doi.org/10.1007/s12035-019-1608-0

Aurora, A. B., & Olson, E. N. (2014). Immune modulation of stem cells and regeneration. *Cell Stem Cell*, *15*, 14–25. https://doi.org/10.1016/j.stem.2014.06.009

Baptista, A. F., Gomes JR de, S., Oliveira, J. T., Santos, S. M. G., Vannier-Santos, M. A., & Martinez, A. M. B. (2007). A new approach to assess function after sciatic nerve lesion in the mouse—Adaptation of the sciatic static index. *Journal of Neuroscience Methods*, *161*, 259–264. https://doi.org/10.1016/j.jneumeth.2006.11.016

Bastien, D., & Lacroix, S. (2014). Cytokine pathways regulating glial and leukocyte function after spinal cord and peripheral nerve injury. *Experimental Neurology*, *258*, 62–77. https://doi.org/10.1016/j.expneurol.2014.04.006

Bell, G. I., Broughton, H. C., Levac, K. D., Allan, D. A., Xenocostas, A., & Hess, D. A. (2011). Transplanted Human Bone Marrow Progenitor Subtypes Stimulate Endogenous Islet Regeneration and Revascularization. https://home.liebertpub.com/scd 21:97–109 Available at: https://www.liebertpub.com/doi/10.1089/scd.2010.0583 [Accessed February 13, 2023].

Bittira, B., Shum-Tim, D., Al-Khaldi, A., & Chiu, R. C.-J. (n.d.). Mobilization and homing of bone marrow stromal cells in myocardial infarction. Available at: www.elsevier.com/locate/ejcts [Accessed February 13, 2023].

Bombeiro, A. L., Lima BH de, M., Bonfanti, A. P., & Oliveira, A. d. (2020). Improved mouse sciatic nerve regeneration following lymphocyte cell therapy. *Molecular Immunology*, *121*, 81–91. https://doi.org/10.1016/j.molimm.2020.03.003

Bombeiro, A. L., Pereira, B. T. N., & de Oliveira, A. L. R. (2018). Granulocyte-macrophage colony-stimulating factor improves mouse peripheral nerve regeneration following sciatic nerve crush. *European Journal of Neuroscience*, *48*, 2152–2164. https://doi.org/10.1111/ejn.14106

Bombeiro, A. L., Santini, J. C., Thomé, R., Ferreira, E. R. L., Nunes, S. L. O., Moreira, B. M., Bonet, I. J. M., Sartori, C. R., Verinaud, L., & Oliveira, A. L. R. (2016). Enhanced immune response in immunodeficient mice improves peripheral nerve regeneration following axotomy. *Frontiers in Cellular Neuroscience*, *10*, 151. https://doi.org/10.3389/fncel.2016.00151

Bouhassira, D., Lantéri-Minet, M., Attal, N., Laurent, B., & Touboul, C. (2008). Prevalence of chronic pain with neuropathic characteristics in the general population. *Pain*, *136*, 380–387. https://doi.org/10.1016/j.pain.2007.08.013

Brenneman, M., Sharma, S., Harting, M., Strong, R., Cox, C. S., Aronowski, J., Grotta, J. C., & Savitz, S. I. (2010). Autologous bone marrow mononuclear cells enhance recovery after acute ischemic stroke in young and middle-aged rats. *Journal of Cerebral Blood Flow & Metabolism*, *30*, 140–149. https://doi.org/10.1038/jcbfm.2009.198

Brini, A. T., Amodeo, G., Ferreira, L. M., Milani, A., Niada, S., Moschetti, G., Franchi, S., Borsani, E., Rodella, L. F., Panerai, A. E., & Sacerdote, P. (2017). Therapeutic effect of human adipose-derived stem cells and their secretome in experimental diabetic pain. *Scientific Reports*, *7*, 1–15. https://doi.org/10.1038/s41598-017-09487-5

Brosius Lutz, A., Lucas, T. A., Carson, G. A., Caneda, C., Zhou, L., Barres, B. A., Buckwalter, M. S., & Sloan, S. A. (2022). An RNA-sequencing transcriptome of the rodent Schwann cell response to peripheral nerve injury. *Journal of Neuroinflammation*, *19*, 1–15. https://doi.org/10.1186/s12974-022-02462-6

Büttner, R., Schulz, A., Reuter, M., Akula, A. K., Mindos, T., Carlstedt, A., Riecken, L. B., Baader, S. L., Bauer, R., & Morrison, H. (2018). Inflammaging impairs peripheral nerve maintenance and regeneration. *Aging Cell*, *17*, e12833. https://doi.org/10.1111/acel.12833

Canè, S., Ugel, S., Trovato, R., Marigo, I., De Sanctis, F., Sartoris, S., & Bronte, V. (2019). The endless saga of monocyte diversity. *Frontiers in Immunology*, *10*, 1–18. https://doi.org/10.3389/fimmu.2019.01786

Caplan, A. I., & Sorrell, J. M. (2015). The MSC curtain that stops the immune system. *Immunology Letters*, *168*, 136–139. https://doi.org/10.1016/j.imlet.2015.06.005

Catenaccio, A., Llavero Hurtado, M., Diaz, P., Lamont, D. J., Wishart, T. M., & Court, F. A. (2017). Molecular analysis of axonal-intrinsic and glial-associated co-regulation of axon degeneration. *Cell Death & Disease 8*:e3166 Available at: www.nature.com/cddis [Accessed November 4, 2020].

Chernov, A. V., Hullugundi, S. K., Eddinger, K. A., Dolkas, J., Remacle, A. G., Angert, M., James, B. P., Yaksh, T. L., Strongin, A. Y., & Shubayev, V. I. (2020). A myelin basic protein fragment induces sexually dimorphic transcriptome signatures of neuropathic pain in mice. *Journal of Biological Chemistry*, *295*, 10807–10821. https://doi.org/10.1074/jbc.RA120.013696

Chernov, A. V., & Shubayev, V. I. (2021). Sexual dimorphism of early transcriptional reprogramming in dorsal root ganglia after peripheral nerve injury. *Frontiers in Molecular Neuroscience*, *14*, 1–16. https://doi.org/10.3389/fnmol.2021.779024

Clements, M. P., Byrne, E., Camarillo Guerrero, L. F., Cattin, A. L., Zakka, L., Ashraf, A., Burden, J. J., Khadayate, S., Lloyd, A. C., Marguerat, S., & Parrinello, S. (2017). The wound microenvironment reprograms Schwann cells to invasive mesenchymal-like cells to drive peripheral nerve regeneration. *Neuron*, *96*, 98–114.e7. https://doi.org/10.1016/j.neuron.2017.09.008

D'Antonio, M., Droggiti, A., Feltri, M. L., Roes, J., Wrabetz, L., Mirsky, R., & Jessen, K. R. (2006). TGFβ type II receptor signaling controls Schwann cell death and proliferation in developing nerves. *The Journal of Neuroscience*, *26*, 8417–8427. https://doi.org/10.1523/JNEUROSCI.1578-06.2006

DeFrancesco-Lisowitz, A., Lindborg, J. A., Niemi, J. P., & Zigmond, R. E. (2015). The neuroimmunology of degeneration and regeneration in the peripheral nervous system. *Neuroscience*, *302*, 174–203. https://doi.org/10.1016/j.neuroscience.2014.09.027

Dhaka, A., Viswanath, V., & Patapoutian, A. (2006). TRP ion channels and temperature sensation. *Annual Review of Neuroscience*, *29*, 135–161. https://doi.org/10.1146/annurev.neuro.29.051605.112958

Evangelista, A. F., Vannier-Santos, M. A., de, A., Silva, G. S., Silva, D. N., Juiz, P. J. L., Nonaka, C. K. V., dos Santos, R. R., Soares, M. B. P., & Villarreal, C. F. (2018). Bone marrow-derived mesenchymal stem/stromal cells reverse the sensorial diabetic neuropathy via modulation of spinal neuroinflammatory cascades. *Journal of Neuroinflammation*, *15*, 189. https://doi.org/10.1186/s12974-018-1224-3

Fillingim, R. B., King, C. D., Ribeiro-Dasilva, M. C., Rahim-Williams, B., & Riley, J. L. (2009). Sex, gender, and pain: A review of recent clinical and experimental findings. *The Journal of Pain*, *10*, 447–485. https://doi.org/10.1016/j.jpain.2008.12.001

Geuna, S. (2015). The sciatic nerve injury model in pre-clinical research. *Journal of Neuroscience Methods*, *243*, 39–46. https://doi.org/10.1016/j.jneumeth.2015.01.021

Goel, R. K., Suri, V., Suri, A., Sarkar, C., Mohanty, S., Sharma, M. C., Yadav, P. K., & Srivastava, A. (2009). Effect of bone marrow-derived mononuclear cells on nerve regeneration in the transection model of the rat sciatic nerve. *Journal of Clinical Neuroscience*, *16*, 1211–1217. https://doi.org/10.1016/j.jocn.2009.01.031

Gomez-Sanchez, J. A., et al. (2015). Schwann cell autophagy, myelinophagy, initiates myelin clearance from injured nerves. *Journal of Cell Biology*, *210*, 153–168. https://doi.org/10.1083/jcb.201503019

Hidmark, A. S., Nawroth, P. P., & Fleming, T. (2017). Analysis of immune cells in single sciatic nerves and dorsal root ganglion from a single mouse using flow cytometry. *Journal of Visualized Experiments*, *6*, 56538–56545. https://doi.org/10.3791/56538

Hong, S., Remacle, A. G., Shiryaev, S. A., Choi, W., Hullugundi, S. K., Dolkas, J., Angert, M., Nishihara, T., Yaksh, T. L., Strongin, A. Y., & Shubayev, V. I. (2017). Reciprocal relationship between membrane type 1 matrix metalloproteinase and the algesic peptides of myelin basic protein contributes to chronic neuropathic pain. *Brain, Behavior, and Immunity*, *60*, 282–292. https://doi.org/10.1016/j.bbi.2016.11.003

Hsieh, C. H., Rau, C. S., Kuo, P. J., Liu, S. H., Wu, C. J., Lu, T. H., Wu, Y. C., & Lin, C. W. (2017). Knockout of toll-like receptor impairs nerve regeneration after a crush injury. *Oncotarget*, *8*, 80741–80756. https://doi.org/10.18632/oncotarget.20206

Huh, Y., Ji, R. R., & Chen, G. (2017). Neuroinflammation, bone marrow stem cells, and chronic pain. *Frontiers in Immunology*, *8*. https://doi.org/10.3389/fmmu.2017.01014.eCollection2017

Jessen, K. R., & Arthur-Farraj, P. (2019). Repair Schwann cell update: Adaptive reprogramming, EMT, and stemness in regenerating nerves. *Glia*, *67*, 421–437. https://doi.org/10.1002/glia.23532

Jessen, K. R., & Mirsky, R. (2016). The repair Schwann cell and its function in regenerating nerves. *The Journal of Physiology*, *594*, 3521–3531. https://doi.org/10.1113/JP270874

Kalinski, A. L., Yoon, C., Huffman, L. D., Duncker, P. C., Kohen, R., Passino, R., Hafner, H., Johnson, C., Kawaguchi, R., Carbajal, K. S., Jara, J. S., Hollis, E., Geschwind, D. H., Segal, B. M., & Giger, R. J. (2020). Analysis of the immune response to sciatic nerve injury identifies efferocytosis as a key mechanism of nerve debridement. *Elife*, *9*, 1–41. https://doi.org/10.7554/eLife.60223

Kavanagh, D. P. J., & Kalia, N. (2011). Hematopoietic stem cell homing to injured tissues. *Stem Cell Reviews and Reports*, *7*, 672–682. Available at: https://link.springer.com/article/10.1007/s12015-011-9240-z [Accessed February 13, 2023]. https://doi.org/10.1007/s12015-011-9240-z

Kigerl, K. A., Gensel, J. C., Ankeny, D. P., Alexander, J. K., Donnelly, D. J., & Popovich, P. G. (2009). Identification of two distinct macrophage subsets with divergent effects causing either neurotoxicity or regeneration in the injured mouse spinal cord. *The Journal of Neuroscience*, *29*, 13435–13444. https://doi.org/10.1523/JNEUROSCI.3257-09.2009

Kim, H., Park, J. S., Yong, J. C., Kim, M. O., Yang, H. H., Kim, S. W., Ji, W. H., Lee, J. Y., Kim, S., Houge, M. A., Ii, M., & Yoon, Y. S. (2009). Bone marrow mononuclear cells have neurovascular tropism and improve diabetic neuropathy. *Stem Cells (Dayton, Ohio)*, *27*, 1686–1696. https://doi.org/10.1002/stem.87

Klein, D., & Martini, R. (2016). Myelin and macrophages in the PNS: An intimate relationship in trauma and disease. *Brain Research*, *1641*, 130–138. https://doi.org/10.1016/j.brainres.2015.11.033

Kobashi, S., Terashima, T., Katagi, M., Nakae, Y., Okano, J., Suzuki, Y., Urushitani, M., & Kojima, H. (2020). Transplantation of M2-deviated microglia promotes recovery of motor function after spinal cord injury in mice. *Molecular Therapy*, *28*, 254–265. https://doi.org/10.1016/j.ymthe.2019.09.004

Kobayashi, H., Chattopadhyay, S., Kato, K., Dolkas, J., Kikuchi, S., Myers, R. R., & Shubayev, V. I. (2008). MMPs initiate Schwann cell-mediated MBP degradation and mechanical nociception after nerve damage. *Molecular and Cellular Neuroscience*, *39*, 619–627. https://doi.org/10.1016/j.mcn.2008.08.008

Kolter, J., Kierdorf, K., & Henneke, P. (2020). Origin and differentiation of nerve-associated macrophages. *The Journal of Immunology*, *204*, 271–279. https://doi.org/10.4049/jimmunol.1901077

Kroner, A., Greenhalgh, A. D., Zarruk, J. G., PassosdosSantos, R., Gaestel, M., & David, S. (2014). TNF and increased intracellular iron alter macrophage polarization to a detrimental M1 phenotype in the injured spinal cord. *Neuron*, *83*, 1098–1116. https://doi.org/10.1016/j.neuron.2014.07.027

Lantero, A., Tramullas, M., Díaz, A., & Hurlé, M. A. (2012). Transforming growth factor-β in normal nociceptive processing and pathological pain models. *Molecular Neurobiology*, *45*, 76–86. https://doi.org/10.1007/s12035-011-8221-1

Leal, M. M. T., Costa-Ferro, Z. S. M., Souza, B. S. D. F., Azevedo, C. M., Carvalho, T. M., Kaneto, C. M., Carvalho, R. H., Dos Santos, R. R., & Soares, M. B. P. (2014). Early transplantation of bone marrow mononuclear cells promotes neuroprotection and modulation of inflammation after status epilepticus in mice by paracrine mechanisms. *Neurochemical Research*, *39*, 259–268. https://doi.org/10.1007/s11064-013-1217-7

Lee, H. J., Remacle, A. G., Hullugundi, S. K., Dolkas, J., Leung, J. B., Chernov, A. V., Yaksh, T. L., Strongin, A. Y., & Shubayev, V. I.

(2022). Sex-specific B cell and anti-myelin autoantibody response after peripheral nerve injury. *Frontiers in Cellular Neuroscience*, *16*, 1–12. https://doi.org/10.3389/fncel.2022.835800.eCollecion2022

Liu, H., Shiryaev, S. A., Chernov, A. V., Kim, Y., Shubayev, I., Remacle, A. G., Baranovskaya, S., Golubkov, V. S., Strongin, A. Y., & Shubayev, V. I. (2012). Innate immunity in multiple sclerosis white matter lesions: Expression of natural cytotoxicity triggering receptor 1 (NCR1). *Journal of Neuroinflammation*, *9*, 1–18. https://doi.org/10.1186/1742-2094-9-1

Liu, P., Peng, J., Han, G. H., Ding, X., Wei, S., Gao, G., Huang, K., Chang, F., & Wang, Y. (2019). Role of macrophages in peripheral nerve injury and repair. *Neural Regeneration Research*, *14*, 1335–1342. https://doi.org/10.4103/1673-5374.253510

L.R. Rilo, H., Cagliani, J., Grande, D., P Molmenti, E., & J. Miller, E. (2017). Immunomodulation by mesenchymal stromal cells and their clinical applications. *Journal Of Stem Cell & Regenerative Biology*, *3*, 1–14. https://doi.org/10.15436/2471-0598.17.022

Luo, X., Chen, O., Wang, Z., Bang, S., Lee, J. J., Huh, S. H., Furutani, Y., He, K., Tao, Q., Ko, X., Bortsov, M. C., Donnelly, A., Chen, C. R., Nackley, Y., Berta, A., Ji, T., & R, R. (2021). IL-23/IL-17A/TRPV1 axis produces mechanical pain via macrophage-sensory neuron crosstalk in female mice. *Neuron*, *109*, 2691–2706.e5. https://doi.org/10.1016/j.neuron.2021.06.015

Lutz, A. B., Chung, W. S., Sloan, S. A., Carson, G. A., Zhou, L., Lovelett, E., Posada, S., Zuchero, J. B., & Barres, B. A. (2017). Schwann cells use TAM receptor-mediated phagocytosis in addition to autophagy to clear myelin in a mouse model of nerve injury. *Proceedings of the National Academy of Sciences of the United States of America*, *114*, E8072–E8080; https://doi.org/10.1073/pnas.1710566114

Macrophages, M.-M.-, Paradigm, T., Mills, C. D., Kincaid, K., Alt, J. M., Heilman, M. J., & Hill, A. M. (2000). M-1/M-2 Macrophages and the Th1/Th2 Paradigm 1.

Mao, H., Wei, W., Fu, X. L., Dong, J. J., Lyu, X. Y., Jia, T., Tang, Y., & Zhao, S. (2019). Efficacy of autologous bone marrow mononuclear cell transplantation therapy in patients with refractory diabetic peripheral neuropathy. *Chinese Medical Journal*, *132*, 11–16. https://doi.org/10.1097/CM9.0000000000000009

Mapplebeck, J. C. S., Beggs, S., & Salter, M. W. (2015). Review articles from the 5th International Meeting of the IASP special interest group on neuropathic pain (NeuPSIG) sex differences in pain: A tale of two immune cells. *Pain*, *157*, 2–6. https://doi.org/10.1097/j.pain.0000000000000389

Marinescu, C. I., Preda, M. B., Neculachi, C. A., Rusu, E. G., Popescu, S., & Burlacu, A. (2021). Identification of a hematopoietic cell population emerging from mouse bone marrow with proliferative potential in vitro and immunomodulatory capacity. *Frontiers in Immunology*, *12*, 1–13; https://doi.org/10.3389/fimmu.2021.698070

Mecklenburg, J., Zou, Y., Wangzhou, A., Garcia, D., Lai, Z., Tumanov, A. V., Dussor, G., Price, T. J., & Akopian, A. N. (2020). Transcriptomic sex differences in sensory neuronal populations of mice. *Scientific Reports*, *10*, 1–18. https://doi.org/10.1038/s41598-020-72285-z

Mietto, B. S., Kroner, A., Girolami, E. I., Santos-Nogueira, E., Zhang, J., & David, S. (2015). Role of IL-10 in resolution of inflammation and functional recovery after peripheral nerve injury. *The Journal of Neuroscience*, *35*, 16431–16442. https://doi.org/10.1523/JNEUROSCI.2119-15.2015

Miller, Y. I., Navia-Pelaez, J. M., Corr, M., & Yaksh, T. L. (2020). Lipid rafts in glial cells: Role in neuroinflammation and pain processing. *Journal of Lipid Research*, *61*, 655–666. https://doi.org/10.1194/jlr.TR119000468

Mills, C. D. (2012). M1 and M2 macrophages: Oracles of health and disease. *Critical Reviews in Immunology*, *32*, 463–488. https://doi.org/10.1615/CritRevImmunol.v32.i6.10

Mogil, J. S., Chesler, E. J., Wilson, S. G., Juraska, J. M., & Sternberg, W. F. (2000). Sex differences in thermal nociception and morphine antinociception in rodents depend on genotype. *Neuroscience & Biobehavioral Reviews*, *24*, 375–389. https://doi.org/10.1016/S0149-7634(00)00015-4

Mokarram, N., Dymanusb, K., Srinivasan, A., Lyon, J. G., Tiptonb, J., Chu, J., English, A. W., & Bellamkonda, R. V. (2017). Immunoengineering nerve repair. *Proceedings of the National Academy of Sciences*, *114*, E5077–E5084. https://doi.org/10.1073/pnas.1705757114

Mokarram, N., Merchant, A., Mukhatyar, V., Patel, G., & Bellamkonda, R. V. (2012). Effect of modulating macrophage phenotype on peripheral nerve repair. *Biomaterials*, *33*, 8793–8801. https://doi.org/10.1016/j.biomaterials.2012.08.050

Muheremu, A., Chen, L., Wang, X., Wei, Y., Gong, K., & Ao, Q. (2017). Chitosan nerve conduits seeded with autologous bone marrow mononuclear cells for 30 mm goat peroneal nerve defect. *Scientific Reports*, *7*, 44002. https://doi.org/10.1038/srep44002

Myers, R. R., & Shubayev, V. I. (2011). The ology of neuropathy: An integrative review of the role of neuroinflammation and TNF-α axonal transport in neuropathic pain. *Journal of the Peripheral Nervous System*, *16*, 277–286. https://doi.org/10.1111/j.1529-8027.2011.00362.x

Nadeau, S., Filali, M., Zhang, J., Kerr, B. J., Rivest, S., Soulet, D., Iwakura, Y., Vaccari, J. P., de, R., Keane, R. W., & Lacroix, S. (2011). Functional recovery after peripheral nerve injury is dependent on the pro-inflammatory cytokines IL-1β and TNF: Implications for neuropathic pain. *The Journal of Neuroscience*, *31*, 12533–12542. Available at: https://www.jneurosci.org/content/31/35/12533 [Accessed July 7, 2020]. https://doi.org/10.1523/JNEUROSCI.2840-11.2011

Naruse, K., Sato, J., Funakubo, M., Hata, M., Nakamura, N., Kobayashi, Y., Kamiya, H., Shibata, T., Kondo, M., Himeno, T., Matsubara, T., Oiso, Y., & Nakamura, J. (2011). Transplantation of bone marrow-derived mononuclear cells improves mechanical hyperalgesia, cold allodynia and nerve function in diabetic neuropathy. *PLoS One*, *6*, e27458. https://doi.org/10.1371/journal.pone.0027458

Niemi, J. P., Defrancesco-Lisowitz, A., Roldan-Hernandez, L., Lindborg, J. A., Mandell, D., & Zigmond, R. E. (2013). A critical role for macrophages near axotomized neuronal cell bodies in stimulating nerve regeneration. *The Journal of Neuroscience*, *33*, 16236–16248. Available at: https://www.jneurosci.org/content/33/41/16236 [Accessed October 10, 2020]. https://doi.org/10.1523/JNEUROSCI.3319-12.2013

North, R. Y., Li, Y., Ray, P., Rhines, L. D., Tatsui, C. E., Rao, G., Johansson, C. A., Zhang, H., Kim, Y. H., Zhang, B., Dussor, G., Kim, T. H., Price, T. J., & Dougherty, P. M. (2019). Electrophysiological and transcriptomic correlates of neuropathic pain in human dorsal root ganglion neurons. *Brain*, *142*, 1215–1226. https://doi.org/10.1093/brain/awz063

Paige, C., Barba-Escobedo, P. A., Mecklenburg, J., Patil, M., Goffin, V., Grattan, D. R., Dussor, G., Akopian, A. N., & Price, T. J. (2020). Neuroendocrine mechanisms governing sex differences in hyperalgesic priming involve prolactin receptor sensory neuron signaling. *The Journal of Neuroscience*, *40*, 7080–7090. https://doi.org/10.1523/JNEUROSCI.1499-20.2020

Pannell, M., Labuz, D., Celik, M., Keye, J., Batra, A., Siegmund, B., & Machelska, H. (2016). Adoptive transfer of M2 macrophages reduces neuropathic pain via opioid peptides. *Journal of Neuroinflammation*, *13*, 262–278. https://doi.org/10.1186/s12974-016-0735-z

Park, J., Zhang, Y., Saito, E., Gurczynski, S. J., Moore, B. B., Cummings, B. J., Anderson, A. J., & Shea, L. D. (2019). Intravascular innate immune cells reprogrammed via intravenous nanoparticles to promote functional recovery after spinal cord injury. *Proceedings of the National Academy of Sciences*, *116*, 14947–14954. https://doi.org/10.1073/pnas.1820276116

Peluffo, H., Solari-Saquieres, P., Negro-Demontel, M. L., Francos-Quijorna, I., Navarro, X., López-Vales, R., Sayós, J., & Lago, N. (2015). CD300f immunoreceptor contributes to peripheral nerve regeneration by the modulation of macrophage inflammatory phenotype. *Journal of Neuroinflammation*, *12*:145–159. https://doi.org/10.1186/s12974-015-0364-y

Perrin, F. E., Lacroix, S., Avilés-Trieueros, M., & David, S. (2005). Involvement of monocyte chemoattractant protein-1, macrophage inflammatory protein-1 and interleukin-1 in Wallerian degeneration. *Brain*, *128*, 854–866. https://doi.org/10.1093/brain/awh407

Piñero, G., Usach, V., Soto, P. A., Monje, P. V., & Setton-Avruj, P. (2018). EGFP transgene: A useful tool to track transplanted bone marrow mononuclear cell contribution to peripheral remyelination. *Transgenic Research*, *27*, 135–153. https://doi.org/10.1007/s11248-018-0062-5

Qu, G., Xie, X., Li, X., Chen, Y., Isla, N. D., Huselstein, C., Stoltz, J.-F., & Li, Y. (2018). Immunomodulatory function of mesenchymal stem cells: Regulation and application. *Journal of Cellular Immunotherapy*, *4*, 1–3. https://doi.org/10.1016/j.jocit.2018.09.001

Ramachandran, R., Wang, Z., Saavedra, C., DiNardo, A., Corr, M., Powell, S. B., & Yaksh, T. L. (2019). Role of toll-like receptor 4 signaling in mast cell-mediated migraine pain pathway. *Molecular Pain*, *15*, 174480691986784. https://doi.org/10.1177/1744806919867842

Rath, M., Müller, I., Kropf, P., Closs, E. I., & Munder, M. (2014). Metabolism via arginase or nitric oxide synthase: Two competing arginine pathways in macrophages. *Frontiers in Immunology*, *5*, 1–11. https://doi.org/10.3389/fimmu.2014.00532

Ray, P. R., Khan, J., Wangzhou, A., Tavares-Ferreira, D., Akopian, A. N., Dussor, G., & Price, T. J. (2019). Transcriptome analysis of the human tibial nerve identifies sexually dimorphic expression of genes involved in pain, inflammation, and neuro-immunity. *Frontiers in Molecular Neuroscience*, *12*, 1–15. https://doi.org/10.3389/fnmol.2019.00037

Ribeiro-Resende, V. T., Carrier-Ruiz, A., Lemes, R. M. R., Reis, R. A. M., & Mendez-Otero, R. (2012). Bone marrow-derived fibroblast growth factor-2 induces glial cell proliferation in the regenerating peripheral nervous system. *Molecular Neurodegeneration*, *7*, 34. https://doi.org/10.1186/1750-1326-7-34

Ribeiro-Resende, V. T., Pimentel-Coelho, P. M., Mesentier-Louro, L. A., Mendez, R. M. B., Mello-Silva, J. P. C., Cabral-da-Silva, M. C., de Mello, F. G., de Melo Reis, R. A., & Mendez-Otero, R. (2009). Trophic activity derived from bone marrow mononuclear cells increases peripheral nerve

regeneration by acting on both neuronal and glial cell populations. *Neuroscience*, *159*, 540–549. https://doi.org/10.1016/j.neuroscience.2008.12.059

Rotshenker, S. (2011). Wallerian degeneration: The innate-immune response to traumatic nerve injury. J Neuroinflammation 8 Available at: https://pubmed.ncbi.nlm.nih.gov/21878125/ [Accessed October 10, 2020].

Savastano, L. E., Laurito, S. R., Fitt, M. R., Rasmussen, J. A., Polo, G., Patterson, V., & I, S. (2014). Sciatic nerve injury: A simple and subtle model for investigating many aspects of nervous system damage and recovery. *Journal of Neuroscience Methods*, *227*, 166–180. https://doi.org/10.1016/j.jneumeth.2014.01.020

Schäfer, M., Fruttiger, M., Montag, D., Schachner, M., & Martini, R. (1996). Disruption of the gene for the myelin-associated glycoprotein improves axonal regrowth along myelin in C57BL/Wlds mice. *Neuron*, *16*, 1107–1113. https://doi.org/10.1016/S0896-6273(00)80137-3

Scholz, J., & Woolf, C. J. (2007). The neuropathic pain triad: Neurons, immune cells and glia. *Nature Neuroscience*, *10*, 1361–1368. Available at: https://www.nature.com/articles/nn1992 [Accessed October 10, 2020]. https://doi.org/10.1038/nn1992

Setton-Avruj, C. P., Musolino, P. L., Salis, C., Alló, M., Bizzozero, O., Villar, M. J., Soto, E. F., & Pasquini, J. M. (2007). Presence of α-globin mRNA and migration of bone marrow cells after sciatic nerve injury suggests their participation in the degeneration/regeneration process. *Experimental Neurology*, *203*, 568–578. https://doi.org/10.1016/j.expneurol.2006.09.024

Shen, Y. J., DeBellard, M. E., Salzer, J. L., Roder, J., & Filbin, M. T. (1998). Myelin-associated glycoprotein in myelin and expressed by Schwann cells inhibits axonal regeneration and branching. *Molecular and Cellular Neuroscience*, *12*, 79–91. https://doi.org/10.1006/mcne.1998.0700

Soto, P. A., Vence, M., Piñero, G. M., Coral, D. F., Usach, V., Muraca, D., Cueto, A., Roig, A., van Raap, M. B. F., & Setton-Avruj, C. P. (2021). *Sciatic nerve regeneration after traumatic injury using magnetic targeted adipose-derived mesenchymal stem cells*. Acta Biomater.

Sta, M., Cappaert, N. L. M., Ramekers, D., Baas, F., & Wadman, W. J. (2014). The functional and morphological characteristics of sciatic nerve degeneration and regeneration after crush injury in rats. *Journal of Neuroscience Methods*, *222*, 189–198. https://doi.org/10.1016/j.jneumeth.2013.11.012

Stephens, K., Zhou, W., Ji, Z., He, S., Ji, J., Guan, Y., & Taverna, S. (2018). Sex differences in gene regulation in the dorsal root ganglion after nerve injury. *The Journal of Pain*, *19*, S100. https://doi.org/10.1016/j.jpain.2017.12.225

Stokes, J. A., Cheung, J., Eddinger, K., Corr, M., & Yaksh, T. L. (2013). Toll-like receptor signaling adapter proteins govern spread of neuropathic pain and recovery following nerve injury in male mice. *Journal of Neuroinflammation*, *10*, 10–13. https://doi.org/10.1186/1742-2094-10-148

Stratton, J. A., Holmes, A., Rosin, N. L., Sinha, S., Vohra, M., Burma, N. E., Trang, T., Midha, R., & Biernaskie, J. (2018).

Macrophages regulate Schwann cell maturation after nerve injury. *Cell Reports*, *24*, 2561–2572.e6. https://doi.org/10.1016/j.celrep.2018.08.004

Takahashi, A., Nakajima, H., Uchida, K., Takeura, N., Honjoh, K., Watanabe, S., Kitade, M., Kokubo, Y., Johnson, W. E. B., & Matsumine, A. (2018). Comparison of mesenchymal stromal cells isolated from murine adipose tissue and bone marrow in the treatment of spinal cord injury. *Cell Transplantation*, *27*, 1126–1139. https://doi.org/10.1177/0963689718780309

Usach, V., Goitia, B., Lavalle, L., Martinez Vivot, R., & Setton-Avruj, P. (2011). Bone marrow mononuclear cells migrate to the demyelinated sciatic nerve and transdifferentiate into Schwann cells after nerve injury: Attempt at a peripheral nervous system intrinsic repair mechanism. *Journal of Neuroscience Research*, *89*, 1203–1217. https://doi.org/10.1002/jnr.22645

Usach, V., Malet, M., López, M., Lavalle, L., Piñero, G., Saccoliti, M., Cueto, A., Brumovsky, P., Brusco, A., & Setton-Avruj, P. (2017). Systemic transplantation of bone marrow mononuclear cells promotes axonal regeneration and analgesia in a model of Wallerian degeneration. *Transplantation*, *101*, 1573–1586. https://doi.org/10.1097/TP.0000000000001478

Ydens, E., Cauwels, A., Asselbergh, B., Goethals, S., Peeraer, L., Lornet, G., Almeida-Souza, L., Van Ginderachter, J. A., Timmerman, V., & Janssens, S. (2012). Acute injury in the peripheral nervous system triggers an alternative macrophage response. *Journal of Neuroinflammation*, *9*, 176–192. https://doi.org/10.1186/1742-2094-9-176

Zaverucha-do-Valle, C., Gubert, F., Bargas-Rega, M., Coronel, J. L. L., Mesentier-Louro, L. A., Mencalha, A., Abdelhay, E., Santiago, M. F., & Mendez-Otero, R. (2011). Bone marrow mononuclear cells increase retinal ganglion cell survival and axon regeneration in the adult rat. *Cell Transplantation*, *20*, 391–406. https://doi.org/10.3727/096368910X524764

Zaverucha-do-Valle, C., Mesentier-Louro, L., Gubert, F., Mortari, N., Padilha, A. B., Paredes, B. D., Mencalha, A., Abdelhay, E., Teixeira, C., Ferreira, F. G. M., Tovar-Moll, F., de Souza, S. A. L., Gutfilen, B., Mendez-Otero, R., & Santiago, M. F. (2014). Sustained effect of bone marrow mononuclear cell therapy in axonal regeneration in a model of optic nerve crush. *Brain Research*, *1587*, 54–68. https://doi.org/10.1016/j.brainres.2014.08.070

Zhan, C., Ma, CB., Yuan, H. M., Cao, B. Y., & Zhu, J. J. (2015). Macrophage-derived microvesicles promote proliferation and migration of Schwann cell on peripheral nerve repair. *Biochemical and Biophysical Research Communications*, *468*, 343–348. https://doi.org/10.1016/j.bbrc.2015.10.097

Zhang, R., Liu, Y., Yan, K., Chen, L., Chen, X. R., Li, P., Chen, F. F., & Jiang, X. D. (2013). Anti-inflammatory and immunomodulatory mechanisms of mesenchymal stem cell transplantation in experimental traumatic brain injury. *Journal of Neuroinflammation*, *10*, 106–117. https://doi.org/10.1186/1742-2094-10-106

Zigmond, R. E., & Echevarria, F. D. (2019). Macrophage biology in the peripheral nervous system after injury. *Progress in Neurobiology*, *173*, 102–121. https://doi.org/10.1016/j.pneurobio.2018.12.001